Analysis of AtGH3.10 for its functions in wound stress response and flower development in *Arabidopsis thaliana*

Jay Camisora Delfin

Nara Institute of Science and Technology
Division of Biological Science

Plant Metabolic Regulation Laboratory
Taku Demura, Ph.D.

2023 January 24

TABLE OF CONTENTS

RESULTS

DISCUSSION

LIST OF TABLES

LIST OF FIGURES

ABSTRACT

Jasmonoyl-isoleucine (JA-Ile) is a key signaling molecule that activates jasmonate-regulated flower development and wound stress response. For years, the JASMONATE RESISTANT1 (JAR1) has been the sole jasmonoyl-amino acid synthetase known to conjugate jasmonic acid (JA) to isoleucine and the source of persisting JA-Ile in *jar1* knockout mutants has remained elusive until now. This study has demonstrated, through recombinant enzyme assays and loss-of-function mutant analyses, that AtGH3.10 functions as a JA-amido synthetase.

Comprehensive phylogenetic analysis of 288 AtJAR1 orthologous proteins from 72 plant species, complemented with synteny analysis, confirmed the long history of divergence of AtGH3.10-like sequences from AtJAR1-like sequences that could be traced back to the early emergence of flowering plants. Limited distribution of the AtGH3.10-like sequences to the angiosperm group particularly in eudicot species was also observed.

Enzyme activity assay of recombinant AtGH3.10 revealed that the enzyme could conjugate JA to isoleucine, alanine, leucine, methionine, and valine. Moreover, kinetic analysis demonstrated that the recombinant AtGH3.10 was more receptive to the five amino acids tested than the recombinant AtJAR1 which could be attributed to the higher specific activity of AtGH3.10 than AtJAR1 observed in isoleucine-limited reaction condition. The AtJAR1, however, had higher affinity and specific activity to JA than AtGH3.10 in *in vitro* reaction.

In vivo analysis established the JA-Ile–biosynthetic function of AtGH3.10. The JA-Ile accumulation in *gh3.10-2 jar1-11* double mutant was nearly eliminated in the leaves and flower buds while its catabolism derivative, 12OH-JA-Ile, was undetected in the flower buds and unwounded leaves. Residual levels of JA-Ile, JA-Ala, and JA-Val were nonetheless detected in *gh3.10-2 jar1-11* suggesting the activities of similar promiscuous enzymes that could conjugate amino acids to JA.

The involvement of AtGH3.10 in the plant response to wounding was also confirmed, as the wound-induced accumulation of JA-Ile and 12OH-JA-Ile and the expression of JA-responsive genes *OXOPHYTODIENOIC ACID REDUCTASE3* and *JASMONATE ZIM-DOMAIN1* observed in WT, *gh3.10-1*, and *jar1-11* leaves were effectively abolished in *gh3.10-2 jar1-11*. Notably, the induction of *AtGH3.10* expression following wounding occurred later than *AtJAR1* expression. Furthermore, systemic induction of *AtGH3.10* expression and accumulation of JAs after wounding were also evident and the role of *AtGH3.10* in this response was additionally suggested by the systemic induction of *AtGH3.10* promoter:GUS activity upon distal wounding.

The role of AtGH3.10 in the biosynthesis of bioactive JAs necessary for normal flower development was also demonstrated. Significant number of flowers with retarded stamen filament elongation and anther dehiscence was observed in *gh3.10-2 jar1-11* flowers which resulted to the increased proportion of undeveloped siliques in *gh3.10-2 jar1-11* plants. This floral phenotype was remarkable compared to that of *jar1-11* and could be attributed to the near elimination of the bioactive JAs in the flower buds and the consequent decline of *MYB21* expression that is critical to the normal flower development.

The aforementioned findings conclusively show that *AtGH3.10* contributes to the biosynthesis of bioactive JA-amino acid conjugates and so it functions partially redundant with *AtJAR1* in sustaining the wound stress response and the flower development in Arabidopsis. Further analysis of other jasmonates and their accumulations at a global scale may reveal a unique function of *AtGH3.10* in plants.

Key words: GH3, JA-Ile, jasmonates, jasmonoyl-amido synthetase, wound response

INTRODUCTION

1.0 Background of the Study

1.1 Jasmonates: physiological roles and signaling mechanism

Jasmonates (JAs) are a group of oxylipin-derived signaling molecules that mediate many aspects of plant processes such as flower development, root growth, trichome formation, anthocyanin production, and leaf senescence. These bioactive molecules are also produced markedly upon abiotic or biotic stresses such as wounding, insect herbivory, and pathogen infection (Wasternack and Hause, 2013; Wasternack and Feussner, 2018). Jasmonates are initially synthesized as jasmonic acid (JA) through a series of enzyme-catalyzed oxidations and reductions of plastid-derived linolenic acid. JA is then converted into different derivatives by, but not limited to, methylation (methyl-jasmonate), hydroxylation (12-OH-JA), decarboxylation (*cis*-jasmone), sulfonation (12-HSO_4-JA), glucosylation (12-*O*-glucosyl-JA, JA-glucosyl-ester), or conjugation to amino acids (Wasternack and Hause, 2013; Fig. 1). These modifications of JA into various jasmonates are thought to determine their bioactivities and metabolic fates, such that hydroxylation and glucosylation may inactivate JA signaling (Miersch *et al.*, 2008; Koo *et al.*, 2011), promote tuber formation (Yoshihara *et al.*, 1989), or facilitate JA transport during a wound response (Glauser *et al.*, 2008). Furthermore, the conjugation of the amino acid isoleucine (Ile) to JA confers major bioactivity and is central to JA signaling and responses.

Among the numerous chemical forms of jasmonates, the (+)-7-*iso*-jasmonoyl-L-isoleucine (JA-Ile) acts as the primary endogenous signal (Fonseca *et al.*, 2009). It is spontaneously converted into its isomer (–)-JA-Ile [or (–)-*trans*-JA-Ile] upon extraction and hence the mixture of them is usually regarded as the natural isomers of JA-Ile. JA-Ile is synthesized by JASMONATE RESISTANT1 (JAR1), an adenylate-forming enzyme that belongs to the Gretchen Hagen3 (GH3) family of acyl acid-amido synthetases in plants (Staswick *et al.*, 2002; Staswick and Tiryaki, 2004; Shimizu *et al.*, 2013). JAR1 has been characterized in *Arabidopsis thaliana* (Staswick *et al.*, 2002; Staswick and Tiryaki, 2004), *Oryza* *sativa* (Riemann *et al.*, 2008; Wakuta *et al.*, 2011; Shimizu *et al.*, 2013), *Selaginella moellendorfffii* (Pratiwi *et al.*, 2017), *Solanum lycopersicum* (Suza *et al.*, 2010), and *Vitis vinifera* (Bottcher *et al.*, 2015). Under normal conditions, JA-Ile is tightly maintained at very low levels to prevent the activation of defense response that antagonizes the plant growth (Yan *et al.*, 2007), but its transient accumulation upon stress like wounding promotes its binding to the co-receptors CORONATINE INSENSITIVE1 (COI1) and JASMONATE ZIM-DOMAIN (JAZ) repressor proteins. COI1, JAZ, and additional components (Sheard *et al.*, 2010) form the SCF^{COI1} E3 ubiquitin ligase complex that tags the JAZ proteins for proteasomal degradation, thereby relieving the transcriptional repression of JA-responsive genes by JAZ (Chini *et al.*, 2007; Thines *et al.*, 2007). The upsurge of JA-Ile upon stress, in turn, is tightly modulated through its conversion to 12OH-JA-Ile by the action of cytochrome P450 enzymes (Koo *et al.*, 2011). The 12OH-JA-Ile, which retains some degree of bioactivity (Jimenez-Aleman *et al.*, 2019; Poudel *et al.*, 2019), is further catabolized into inactive form mainly via two pathways leading to 12COOH-JA-Ile (Heitz *et al.*, 2012; Koo *et al.*, 2014) or 12OH-JA (Widemann *et al.*, 2013).

1.2 JA-biosynthesis and -signaling mutants

Arabidopsis mutant analyses have facilitated the elucidation of the underlying mechanisms of the developmental and physiological roles of jasmonates and its signaling. Loss-of-function mutations in the genes involved in JA biosynthesis such as *ALLENE OXIDE SYNTHASE* (*AOS*) (Park *et al.*, 2002) and *OXOPHYTODIENOIC ACID REDUCTASE3* (*OPR3*) (Chini *et al.*, 2018) or in the COI1-mediated signaling (Xie *et al.*, 1998) result in male-sterile flowers that are characterized by stunted filament elongation, retarded anther dehiscence, and impaired pollen maturation. In addition, these mutants are more susceptible to pathogen infection and wound stress (Koo and Howe, 2009; Howe *et al.*, 2018). The *jar1* mutants, in contrast, are still fertile and have only moderate sensitivity to methyl jasmonate-induced root growth inhibition (Staswick *et al.*, 1992; Staswick *et al.*, 2002) or pathogen infection (Ferrari *et al.*, 2003). Indeed, residual amount of JA-Ile is still detectable in the roots, shoots, and flowers of *jar1* mutants. Upon wounding, the JAs level in *jar1* can be even stimulated modestly and the expression of several wound-responsive genes such as *VSP2* (*VEGETATIVE STORAGE PROTEIN2*), *TAT3* (*TYROSINE AMINOTRANSFERASE3*), *CORI3* (*CORONATINE INDUCIBLE3*), *LOX2* (*LIPOXYGENASE2*), and *PDF1.2* (*PLANT DEFENSIN1.2*) are generally unaffected (Staswick and Tiryaki, 2004; Chung *et al.*, 2008; Suza and Staswick, 2008; Yan *et al.*, 2016). Additionally, the amount of JA-Ile in *jar1-1* is only partially affected by a chemical inhibitor of AtJAR1 (Meesters *et al.*, 2014), implying that a similar JA-amido synthetase with slightly different acyl acid binding site exists. This moderate phenotypes of *jar1* mutants and its hitherto unknown source of the residual JA-Ile suggest the presence of an alternative JA-Ile biosynthetic enzyme other than JAR1 in Arabidopsis.

1.3 GH3 family of phytohormone-modifying enzymes

The plant GH3 enzymes belong to a firefly luciferase-like superfamily and chemically modify phytohormones like jasmonates, auxins, or benzoate derivatives (Staswick *et al.*, 2002; Staswick *et al.*, 2005; Okrent *et al.*, 2009; Wojtaczka *et al.*, 2022). These enzymes employ a two-step mechanism involving adenylation and transferase activities to conjugate several amino acids to phytohormones (Westfall *et al.*, 2012), thereby altering the physiological activities of the latter. Unlike the amide conjugates of auxins that are inactive and serve as the storage forms of the hormone, the JA-amido conjugates are mainly the bioactive form of this hormone.

Phylogenetic analyses have grouped the plant GH3 genes into three major clades corresponding to the type of substrate specific to each clade. The Group I of the GH3 family is associated with JA-amino acid conjugation and is comprised of two members in *A. thaliana*, namely *AtGH3.11/AtJAR1* and *AtGH3.10/DWARF IN LIGHT2* (*DFL2*). However, previous phylogenetic and sequence analyses suggest that the two genes can be separated into two subgroups (Okrent and Wildermuth, 2011; Westfall *et al.*, 2012).

1.4 JAR1 in plant processes and the putative role of GH3.10

Aside from its pivotal role in jasmonate biosynthesis and thus signaling, AtJAR1 is also associated with plant development. When grown in far-red (FR) and low fluence red light, *jar1* mutants exhibit long hypocotyls while an opposite phenotype is observed in blue light (Chen *et al.*, 2007; Wang *et al.*, 2011; Chen *et al.*, 2018). Interestingly, this light-related function of AtJAR1 is based on its physical interaction with specific proteins. AtJAR1 (also known as FAR-RED INSENSITIVE219, FIN219) binds a FIN219-interacting protein (FIP1), a glutathione *S*-transferase, on its C-terminal domain which consequently enhances its JA-Ile biosynthetic activity under phytochrome A-dependent FR light signaling (Chen *et al.*, 2007; Chen *et al.*, 2018). Moreover, AtJAR1 also binds to the C-terminal domain of CONSTITUTIVE PHOTOMORPHOGENIC1 (COP1) to modulate its subcellular localization and to negatively regulate its activity under dark and continuous FR conditions (Wang *et al.*, 2011). These interactions seem to suggest a non-enzymatic function of AtJAR1 in mediating a crosstalk between jasmonate signaling and plant processes such as photomorphogenesis and abiotic stress response.

On the other hand, the overexpression of *AtGH3.10* results in a short hypocotyl under red and blue light, whereas the anti-sensed gene results in a long hypocotyl under red light (Takase *et al.*, 2003). To date, this is the only report that characterized a possible function of *AtGH3.10*. Despite its predicted phylogenetic-based functional attributes, the enzyme product of *AtGH3.10* was found to be inactive in *in vitro* studies and thus its involvement in JA-Ile biosynthesis has been disregarded (Staswick *et al.*, 2002; Chiu *et al.*, 2018). The existence of another jasmonoyl-amido synthetase in Arabidopsis other than AtJAR1 that is responsible for the persisting levels of JA-Ile in *jar1* mutants has been speculated for years until now.

2.0 Purpose of the Study

This study aimed to demonstrate whether the *AtGH3.10* gene in Arabidopsis encodes an enzyme that functions as JA-amido synthetase. The characterization of the gene's functions involved the following analyses:

1. phylogenetic analysis,
2. *in vitro* recombinant enzyme activity and kinetic assays,
3. knockout mutant analyses including
    a. morphological analysis,
    b. endogenous hormone quantification using LC-MS/MS analysis,
    c. wounding response analysis, and
    d. JA- and light-treatment response experiments.

3.0 Significance of the Study

The functional characterization of AtGH3.10 reveals its important role in the biosynthesis of bioactive JA-Ile and other JA-amido conjugates necessary for JA-mediated processes like wound response and flower development. This helps to explain the *jar1* mutant phenotypes and the generation of *gh3.10 jar1* double mutants could serve as a valuable tool for exploring the functions of various jasmonates, other than their amino acid conjugates, in many JA-mediated developmental processes and stress responses of plants.

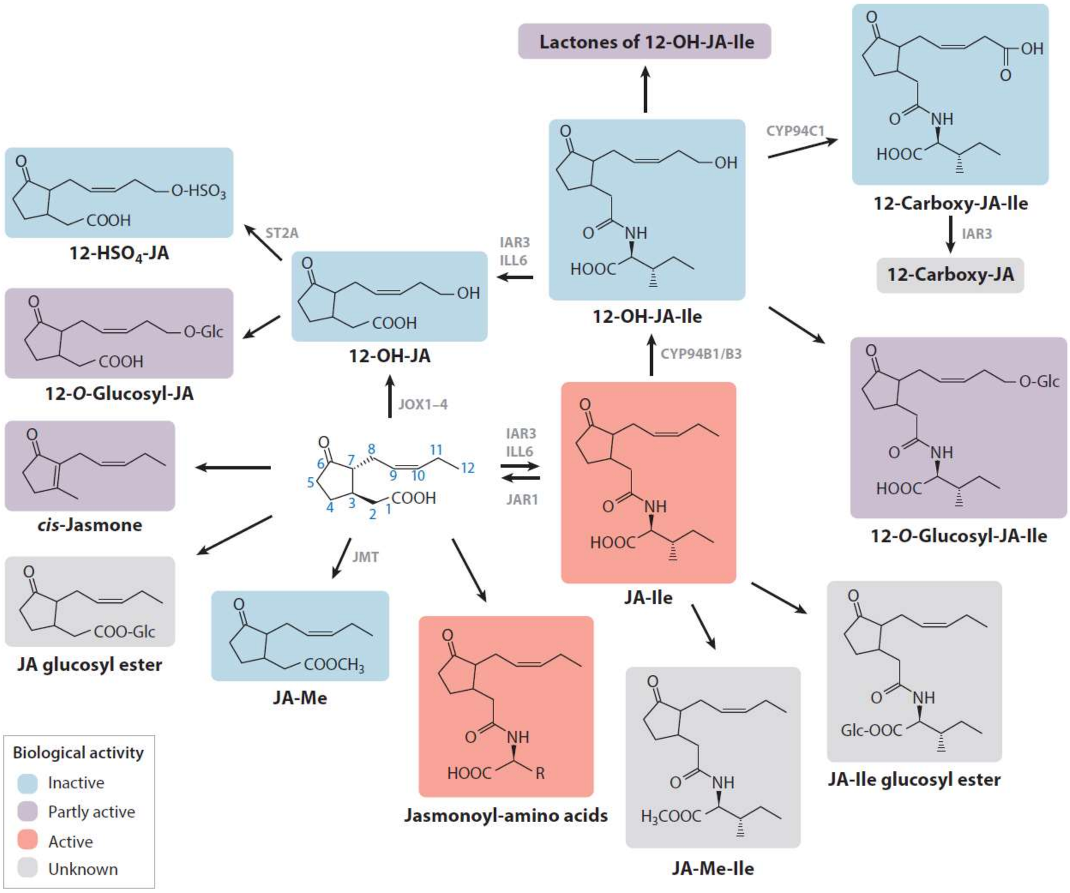

Figure 1. Metabolism of jasmonic acid

Known enzymes involved in the metabolic conversion of JA include: JAR1 (jasmonoyl amino acid conjugate synthase), JA-Ile-12-hydroxylase CYP94B3, 12-OH-JA-Ile carboxylase CYP94C1, amidohydrolases IAR3 and ILL6, jasmonate-induced oxygenases JOX1–4, JMT (JA methyl transferase), and ST2A (12-OH-JA sulfotransferase) (adapted from Wasternack and Feussner, 2018).

MATERIALS AND METHODS

Plant material and growth conditions

Seeds of *Arabidopsis thaliana* (Columbia-0) wild type and *jar1-11* (SALK_034543) were obtained from the Arabidopsis Biological Resource Center. The seeds were soaked in water and vernalized at 4°C for at least three days before sowing on a 1:1 vermiculite: peat moss mix. Plants were grown in a growth chamber with a 16h-light/8h-dark photoperiod at 23°C, with a light intensity of 40 µmol m^{-2} sec^{-1}. Leaf and flower samples for hormone quantification, gene cloning, and expression analyses were harvested, snap-frozen in liquid nitrogen, homogenized using a Tissue Lyser II (Qiagen), and stored at -80°C until use.

Recombinant enzyme assay

The coding sequences of *AtJAR1* and *AtGH3.10* were cloned using KOD Plus Ver. 2 (Toyobo, Osaka, Japan) and separately inserted into pENTR™4 via the SLiCE reaction (Motohashi, 2015). Using Gateway™ LR Clonase™ II enzyme mix (Invitrogen, Waltham, MA, USA), the entry clone was recombined with pDEST™15 that contains a glutathione-*S*-transferase (GST) tag. After confirming the sequence, the vector was introduced into competent SoluBL21™ *E. coli* (Genlantis, San Diego, CA, USA) harboring pRARE, and the transformants were cultured in M9 minimal medium at 28°C with shaking to an OD_{600} >0.4. Protein expression was induced by adding isopropyl β-D-1-thiogalactopyranoside to a final concentration of 1 mM and incubated overnight at 20°C with shaking. Cells were collected via centrifugation at 4°C, dissolved in 5 mL cold lysis buffer (20 mM Tris-HCl, pH 7.5), and crushed by sonication on ice for 1 min. Following centrifugation at 12,000 x *g* for 10 min at 4°C, the lysate's supernatant liquid was collected and analyzed for the presence of recombinant proteins by SDS-PAGE. The GST-tagged AtJAR1 or AtGH3.10 proteins were recovered using Cosmogel® GST-Accept (Nacalai Tesque, Kyoto, Japan) and concentrated in its final suspension buffer (0.1 M sodium phosphate with 10 mM NaCl, pH 7.4) using an Amicon® Ultra-0.5 30K centrifugal filter (Merck, Darmstadt, Germany). Protein concentrations were determined by Bradford assay.

Kinetics assays were carried out in a 50-µL reaction mixture consisting of 181 ng of GST-AtJAR1 or 198 ng of GST-AtGH3.10 (ideally, 2 pmol of each recombinant protein), JA (racemic) at 1 mM or varying concentrations (0.02, 0.04, 0.06, 0.08, and 0.10 mM), L-isoleucine at 1 mM or at varying concentrations as for JA, 1.5 mM $MgCl_2$, 1.5 mM ATP, and 1 mM dithiothreitol, in 0.1 M sodium phosphate buffer (pH 7.0). After 15 min incubation at 23°C, the reaction was stopped by adding 150 µL 10% (v/v) acetic acid. The reaction product was extracted from the mixture using ethyl acetate with 100 pg JA-[$^{13}C_6$]Ile as an internal standard, followed by another round of ethyl acetate extraction. The organic fractions from the two extractions were collected after centrifugation at 11,100 x *g* for 5 min and combined, dried in a rotary evaporator, and stored at -30°C until LC-MS/MS analysis. K_m value was calculated using Michaelis-Menten equation. The concentration of (–)-JA was assumed as one-half the amount of racemic JA. For comparative activity assays of AtGH3.10 and AtJAR1, 1 mM JA, 1 mM amino acid (Ile, Ala, Leu, Met, or Val), and 2 pmol of the enzyme were used. The reaction mixtures were incubated for 43 hours prior to extraction and quantitation of JA-amino acid conjugates.

Generation of knockout mutants

The *gh3.10-1* and *gh3.10-2 jar1-11* mutants were generated from Col-0 and *jar1-11* as parental lines, respectively, using the pKAMA-ITACHI vector-based CRISPR/Cas9 system (Tsutsui and Higashiyama, 2017). Single-guide RNA (sgRNA) for mutating the genomic *AtGH3.10* region was selected through the "CRISPRdirect" website (https://crispr.dbcls.jp) with the ORF sequence of *AtGH3.10* as the query. The double-stranded DNA fragment of the selected sgRNA region (5'-CCATAGCGCGCAAACTACTCTTC-3') with flanking vector sequences for cloning was obtained by annealing two single-stranded DNA fragments (Method Table 1). The double-stranded DNA fragment was inserted into the AarI-digested pKI1.1R using the SLiCE to generate pKI1.1R/AtGH3.10sgRNA that was transfected into Col-0 and *jar1-11* via floral dipping with *Agrobacterium* *tumefaciens* strain GV3101. Transformed seeds containing the CRISPR/Cas9 cassette were selected by observing the seed coat RFP signal. The mutation in *AtGH3.10* in the T_1 generation transgenic plants was confirmed by DNA sequencing (primers 'AtGH3.10_seqF/R'; Fig. 8, Method Table 1). Seeds from the T_2 generation were harvested from homozygotes of the *AtGH3.10* mutations. Seeds without the CRISPR/Cas9 cassette were selected as indicated by the disappearance of the seed coat RFP signal. The T_3 generation of mutants was used for the experiments.

Wounding treatment

Three sets of five-week-old Arabidopsis plants were prepared for three treatments: unwounded, 30-min after wound stress, and 120-min after wound stress. Four rosette leaves per plant were pressed between the serrated tips of forceps at four different sites across the midvein. The wounded leaves were harvested after 30 or 120 minutes after wounding. The harvested leaves were immediately frozen in liquid nitrogen, homogenized, and stored at -80^{o}C until further use.

Hormone extraction and purification from plant tissue

Hormones were extracted from approx. 50 mg of leaf tissues or 15 mg of flower buds using 80% acetonitrile in 1% acetic acid (v/v/v) containing stable isotope-labeled hormones as internal standards ([D_2]JA, JA-[$^{13}C_6$]Ile, 12OH-JA-[$^{13}C_6$]Ile, and JA-[D_3]Ala for buds, and [D_2]JA and JA-[$^{13}C_6$]Ile for leaves). The extracts were purified using OASIS WAX cartridge columns (Waters, Milford, MA, USA) as previously described (Kanno *et al.*, 2016). Hormones were eluted from the cartridge column with 80% acetonitrile containing 1% acetic acid (v/v/v), dried *in vacuo*, and finally resuspended in 1% (v/v) acetic acid.

Hormone measurements by LC-MS/MS

Hormone levels were measured using a Triple TOF 5600 system (SCIEX) combined with a Nexcera HPLC system (Shimadzu, Kyoto, Japan) with a ZORBAX Eclipse XDB-C18 column (Agilent, Santa Clare, CA, USA) as described previously (Kanno *et al.*, 2016) with some modifications. Hormone levels were calculated based on the peak area ratio of detected hormone and stable isotope standard, *i.e.*, JA and JA-Ile were based on appropriate standards; 12OH-JA-Ile and JA-Ala in leaves and JA-Val in leaves and flower buds were quantified relative to JA-[$^{13}C_6$]Ile; 12OH-JA-Ile and JA-Ala in flower buds were quantified based on appropriate standards. The detection of JA-Ile and JA-Leu was further confirmed by separate analysis (Fig. 10). HPLC and mass spectrometer conditions are specified in Method Table 2.

Promoter-GUS assay

A 2-kbp sequence upstream of the *AtGH3.10* coding sequence was initially cloned in pENTR™4 and subcloned into pGWB3 via Gateway™ LR reaction (Invitrogen) to make the *AtGH3.10p::GUS* construct used to transform Col-0 and *jar1-11* (Method Table 1). Whole plant samples were harvested and soaked immediately in cold 90% (v/v) acetone and kept on ice for 15 min. The samples were washed once with GUS buffer containing 100 mM sodium phosphate (pH 7.0), 10 mM EDTA, 0.5 mM potassium ferricyanide, 0.5 mM potassium ferrocyanide, and 0.1% (v/v) Triton X-100. The samples were soaked in staining buffer consisting of 0.5 mg/mL X-gluc in GUS buffer and vacuum infiltrated. After overnight incubation in staining buffer at 37°C, the samples were repeatedly soaked and washed with 70% (v/v) ethanol until the pigments faded.

RNA extraction and RT-qPCR

Total RNA was extracted from 12 mg of powdered plant sample using 0.5 mL of Sepasol®-RNA Super G (Nacalai) following the manufacturer's instructions. The cDNA was then synthesized from 500 ng total RNA using ReverTra Ace® qPCR RT Master Mix with gDNA Remover (Toyobo Co. Ltd.) following the product's protocol. The resulting 10 µL reaction mixture was diluted 40x and used with the Thunderbird™ SYBR™ qPCR Mix (Toyobo) for real-time PCR using CFX Connect™ Real-Time System (Bio-Rad, Hercules, CA, USA). Melting curve analysis was conducted to confirm gene-specific amplification. The cycling conditions consisted of a pre-denaturation step at 95°C for 1 min followed by 40 cycles of denaturation at 95°C for 15 sec, annealing at 52°C for 15 sec, and extension at 72°C for 30 sec. Primer pairs are listed in Method Table 1. The expression levels of target genes were estimated by comparative Ct method using *AtUBQ10* as the reference gene and were expressed as fold difference relative to WT.

Phylogenetic analysis

The initial sequence comparison used 287 amino acid sequences deduced from *AtJAR1* orthologous genes among the 71 plant species found in the PLAZA database (Dicots 4.0 and Monocots 4.5). Sequences of less than 300 amino acids were excluded. Sequence alignment was done in MEGA X (version 10.2.4) using MUSCLE algorithm. Maximum Likelihood (ML) method was used based on the JTT-matrix model with discrete Gamma distribution to model evolutionary rate differences among sites. After confirming the separation of sequences by clades, only 77 amino acid sequences from 40 species representing the major plant taxa were selected for another ML-based tree construction with 1000 bootstrap replications.

Statistical analysis

Differences between means were determined by one-way or two-way ANOVA with appropriate *post hoc* tests, where $p<0.05$ was considered significant. Statistical analyses were carried out using IBM SPSS Statistics v26, and graphs were made using GraphPad Prism v9.0.

Method Table 1. Sequences of primers used in this study

Primer name	Sequence (5'–3')	Purpose
AtGH3.10pro_to_pENTR4 (Nco1)_F	AAAAGCAGGCTCCACCATGGATCAGACTA CATGTTACTTACAACAG	cloning to pENTR4
AtGH3.10pro_to_pENTR4 (Xho1)_R	CTGGGTCTAGATATCTCGACCAATACCAA GTCTTTCAAGGC	cloning to pENTR4
AtGH3.10_qPCR_F2	GGGTTCTATGCTGCCGTAC	qPCR analysis
AtGH3.10_qPCR_R2	GAATCACAGCAAAGCTCACG	qPCR analysis
AtJAR1_qPCR_F	ACAGGGGAAGGAGAGGAGAA	qPCR analysis
AtJAR1-qPCR_R	CACATCTCCAAGCCGGTATC	qPCR analysis
AtJAZ1_qPCR_F	AGCGTCTTCAAACCCTCAAA	qPCR analysis
AtJAZ1_qPCR_R	TGAAGCAACGTCGTCAAAAG	qPCR analysis
OPR3_qPCR_F	TGGACGCAACTGATTCTGAC	qPCR analysis
OPR3_qPCR_R	GCGAGCTTTGAGCCATTAAC	qPCR analysis
AtMYB21_qPCR_F	CACTCCAGAAGAGCAACTTATC	qPCR analysis
AtMYB21_qPCR_R	CATCCGATTGCTTGATGTATTTTTG	qPCR analysis
AtMYB24_qPCR_F	GGGTCTGGATCAGGAGATGC	qPCR analysis
AtMYB24_qPCR_R	CAGGTCGGAGGTAGTTCAGC	qPCR analysis
AtUBQ10_qPCR_F	GGCCTTGTATAATCCCTGATGAATAAG	qPCR analysis
AtUBQ10_qPCR_R	AAAGAGATAACAGGAACGGAAACATAGT	qPCR analysis
AtGH3.10pro_seqF1	GGAGGTAAGATGAGCTGGTG	sequencing promoter
AtJAR1ORF_seqF1	TCAGAAACAGAGATTTTCCC	sequencing ORF
AtJAR1ORF_seqR1	AGCTTTGAAGTTAGGGTTGC	sequencing ORF
AtJAR1ORF_seqF2	CGGTTGGTTTAACTCAAGTC	sequencing ORF
AtJAR1ORF_seqR2	TGTTGATCGAGAGAATCAGG	sequencing ORF
AtGH3.10ORF_seqF1	TCAGCGGCTTACAGATCAAG	sequencing ORF
AtGH3.10ORF_seqR1	CTCTTCGCTCGCATAGTAAT	sequencing ORF
AtGH3.10ORF_seqF2	CAGATTAGGAGACGTAGTTG	sequencing ORF
AtGH3.10ORF_seqR2	CTCTCTGAAGATCCTTCTCT	sequencing ORF
AtGH3.10_sgRNA_F	AGAGTCGAAGTAGTGATTGAAGAGTAGTT TGCGCGCTA	CRISPR mutation
AtGH3.10_sgRNA_R	CTATTTCTAGCTCTAAAACTAGCGCGCAA ACTACTCTTC	CRISPR mutation
AtGH3.10_seqF	TGAAGACAAAGGGAGTGGTCA	sequencing mutation
AtGH3.10_seqR	TGGCTGGAGTAATGGAGACC	sequencing mutation

Method Table 2. HPLC and mass spectrometer conditions used for analysis

Conditions of HPLC					
Method #	Sample	Solvent A	Solvent B	Flow rate (μl min^{-1})	Gradient (composition of solvent B)
1	Plant extract samples (Fig.10) & Enzyme assay samples for determination of affinity to JA and Ile (Fig. 5a)	Water containing 0.01% (v/v) acetic acid	Acetonitrile containing 0.05% (v/v) acetic acid	400	Constant 3% for 0.3 min Linear gradient from 3% to 15% over 0.7 min Constant 15% for 2 min Linear gradient from 15% to 40% over 4 min Linear gradient from 40% to 60% over 1 min
2	Enzyme assay samples for comparison of substrate specificity (Fig. 5C)	Water containing 0.01% (v/v) acetic acid	Acetonitrile containing 0.05% (v/v) acetic acid	400	Constant 3% for 0.5 min Linear gradient from 3% to 70% over 7.5 min
3	Plant extract samples (Fig. 10 for 12OH-JA-Ile, Fig. 11, & Fig.19)	Water containing 0.01% (v/v) acetic acid	Acetonitrile containing 0.05% (v/v) acetic acid	400	Constant 3% for 0.5 min Linear gradient from 3% to 45% over 5.5 min Constant 45% over 1.5 min
4	Peak identification of JA-Ile and JA-Leu (Fig. 9)	Water containing 0.01% (v/v) acetic acid	Acetonitrile containing 0.05% (v/v) acetic acid	200	Constant 30% for 30 min

Conditions of mass spectrometer											
Compound	HPLC method #	Retention time on HPLC (min)	Polarity of ESI	Ion Spray voltage (kV)	Desolvation temperature (°C)	Declus-tering potential (V)	Collision energy (V)	Precursor ion (m/z)	Scan range (m/z)	Qualifier ion (m/z)	Limit of Quantita-tion (pg)
JA	1	6.11	negative	-3.5	600	-90	-20	209.2	50-250	59	1
	3	4.8	negative	-3.5	600	-90	-20	209.2	50-250	59	1
[D_2]JA	1	6.11	negative	-3.5	600	-90	-20	211.2	50-250	59	-
	3	4.79	negative	-3.5	600	-90	-20	211.2	50-250	59	-
(-)-trans-JA-Ile	1	7.38	negative	-3.5	600	-90	-30	322.2	50-350	130.1	0.3
	2	5.40	negative	-4.5	600	-90	-30	322.2	50-500	130.1	0.3
	3	5.64	negative	-4.5	600	-90	-30	322.2	50-500	130.1	0.3
	4	6.72	negative	-4.5	600	-90	-30	322.2	50-500	130.1	-
(+)-cis-JA-Ile	1	7.44	negative	-3.5	600	-90	-30	322.2	50-350	130.1	0.3
	2	5.50	negative	-4.5	600	-90	-30	322.2	50-500	130.1	0.3
	4	7.15	negative	-4.5	600	-90	-30	322.2	50-500	130.1	-
(+)-trans-JA-Ile	1	7.22	negative	-3.5	600	-90	-30	322.2	50-350	130.1	0.3
	2	5.23	negative	-4.5	600	-90	-30	322.2	50-500	130.1	0.3
	3	5.5	negative	-4.5	600	-90	-30	322.2	50-500	130.1	0.3
	4	5.5	negative	-4.5	600	-90	-30	322.2	50-500	130.1	-
(-)-trans-JA-[$^{13}C_6$]Ile	1	7.37	negative	-3.5	600	-90	-30	328.2	50-350	136.1	-
	2	5.40	negative	-4.5	600	-90	-30	328.2	50-500	136.1	-
JA-Leu	2	5.48	negative	-4.5	600	-90	-30	322.2	50-500	130.1	5
	4	7.4	negative	-4.5	600	-90	-30	322.2	50-500	130.1	-
JA-Ala	2	4.14	negative	-4.5	600	-90	-30	280	50-500	88.1	0.5
	3	4.19	negative	-4.5	600	-90	-30	280	50-500	88.1	0.5
JA-[D_3]Ala	3	4.19	negative	-4.5	600	-90	-30	283	50-500	91.1	-
JA-Val	2	4.98	negative	-4.5	600	-90	-30	308	50-500	116.1	0.5
	3	5.13	negative	-4.5	600	-90	-30	308	50-500	116.1	0.5
JA-Met	2	4.9	negative	-4.5	600	-90	-30	340	50-500	148	-
	3	5.09	negative	-4.5	600	-90	-30	340	50-500	148	-
12OH-JA-Ile	3	3.91	negative	-4.5	600	-110	-30	338.2	50-500	130.1	7
12OH-JA-[$^{13}C_6$]Ile	3	3.91	negative	-4.5	600	-110	-30	344.2	50-500	136.1	-

Method Table 3. *P* values obtained from two-way ANOVA

Figure	Data	*P* values		
		Treatment (T)	Genotype (G)	Interaction (I)
8	*AtGH3.10*	2.93E-09	3.58E-05	0.167
	AtJAR1	1.32E-06	< 2.2E-16	0.054
	JAZ1	< 2.2E-16	2.46E-11	2.43E-04
	OPR3	9.84E-16	1.40E-09	4.20E-04
10,11	JA	< 2.2E-16	0.305	9.13E-03
	JA-Ile	5.89E-14	< 2.2E-16	0.580
	12OH-JA-Ile	<0.0001	<0.0001	<0.0001
	JA-Ala	<0.0001	1.00E-03	3.62E-02
	JA-Val	<0.0001	<0.0001	<0.0001

Method Table 4. *AtJAR1* orthologous Arabidopsis genes used in this study

Plant species	Gene ID	Gene name
Actinidia chinensis	Achn042951	
Actinidia chinensis	Achn275921	
Amborella trichopoda	ATR0693G197	
Amborella trichopoda	ATR1100G036	
Ananas comosus	Aco009148	
Ananas comosus	Aco010717	
Ananas comosus	Aco005530	
Arabidopsis thaliana	AT4G03400	*AtGH3.10/DFL2*
Arabidopsis thaliana	AT2G46370	*AtJAR1*
Arabidopsis thaliana	AT3G27810	*AtMYB21*
Arabidopsis thaliana	AT5G40350	*AtMYB24*
Arabidopsis thaliana	AT1G19180	*AtJAZ1*
Arabidopsis thaliana	AT2G06050	*AtOPR3*
Arabidopsis thaliana	AT4G05320	*AtUBQ10*
Arachis ipaensis	Araip.1R458	
Arachis ipaensis	Araip.3EM6P	
Asparagus officinalis	evm.TU.AsparagusV1_03.2206.V1.1	
Asparagus officinalis	evm.TU.AsparagusV1_01.2650.V1.1	
Asparagus officinalis	evm.TU.AsparagusV1_01.334.V1.1	
Azolla filiculoides	Azfi s0155.g053629	
Beta vulgaris	Bv1_003490_qqms	
Brassica oleracea	Bo9g007560	
Brassica oleracea	Bo4g009300	
Calamus simplicifolius	CALSI_Maker00010895	
Calamus simplicifolius	CALSI_Maker00043463	
Carica papaya	Cpa.g.sc34.122	
Carica papaya	Cpa.g.sc1483.1	
Chenopodium quinoa	AUR62037363	
Chenopodium quinoa	AUR62004459	
Citrus clementina	Ciclev10014670m.g	
Citrus clementina	Ciclev10019459m.g	
Coffea canephora	Cc05_g06700	
Coffea canephora	Cc02_g39050	
Cucumis melo	MELO3C013558	
Cucumis melo	MELO3C006046	
Daucus carota	DCAR_012993	
Daucus carota	DCAR_025240	
Elaeis guineensis	p5.00_sc00154_p0063	
Elaeis guineensis	p5.00_sc00050_p0066	
Elaeis guineensis	p5.00_sc00126_p0054	
Eucalyptus grandis	Eucgr.A01790	
Eucalyptus grandis	Eucgr.E00072	
Fragaria vesca	FVE10286	

Glycine max	Glyma.05G034000	
Glycine max	Glyma.03G256200	
Gossypium raimondii	Gorai.002G017500	
Gossypium raimondii	Gorai.007G106500	
Hordeum vulgare	HORVU3Hr1G029670	
Hordeum vulgare	HORVU1Hr1G092890.	
Malus domestica	MDO.mRNA.g.4180.3	
Medicago truncatula	Medtr0102s0060	
Medicago truncatula	Medtr8g027955	
Musa acuminata	Ma01_g04210	
Musa acuminata	Ma04_g08500	
Nelumbo nucifera	NNU_09295	
Nelumbo nucifera	NNU_02472	
Oryza sativa	LOC_Os05g50890	*OsJAR1*
Oryza sativa	LOC_Os01g12160	*OsJAR2*
Oryza sativa	LOC_Os11g08340	*OsJAR3*
Petunia axillaris	Peaxi162Scf01258g00119	
Petunia axillaris	Peaxi162Scf01012g00020	
Phalaenopsis equestris	PEQU_05514	
Phalaenopsis equestris	PEQU_20457	
Physcomitrium patens	Pp3c10_20960	
Picea abies	PAB00039344	
Populus trichocarpa	Potri.019G103500	
Populus trichocarpa	Potri.002G168200	
Selaginella moellendorffii	gene21103	*SmJAR1*
Solanum lycopersicum	Solyc10g008520.2	
Solanum lycopersicum	Solyc10g011660	*SlJAR1*
Tarenaya hassleriana	THA.LOC104815954	
Tarenaya hassleriana	THA.LOC104817340	
Utricularia gibba	UGI.Scf01128.20304	
Vitis vinifera	GSVIVG01027057001	*VvGH3-7*
Vitis vinifera	GSVIVG01030558001	
Zea mays	Zm00001d039345	
Zea mays	Zm00008a030342	
Zea mays	Zm00008a032109	
Zea mays	Zm00008a030883	
Ziziphus jujuba	ZJU.LOC107416751	
Zostera marina	Zosma310g00020	
Zostera marina	Zosma267g00360	

RESULTS

1.0 *AtGH3.10* and *AtJAR1* belong to phylogenetically distinct clades

AtGH3.10 and *AtJAR1* are members of one of the three groups of GH3 gene family in *A. thaliana* based on their deduced amino acid sequences (Fig. 2). This grouping was consistent with the type of substrate that each group utilizes. In addition, subgroups can be distinguished within group I and III when their acyl binding site sequences are considered, as was previously described (Westfall *et al.*, 2012). In Group I, for instance, AtGH3.10 and AtJAR1 are sharing 47.9% amino acid sequence identity and are in separate subgroups due to their acyl binding site sequence differences that are reflected by the large evolutionary distance from their common ancestral sequence, in comparison to those between GH3 members of group II (Fig. 2). To put this into a broader perspective, phylogenetic analysis based on maximum likelihood was initially performed for 287 protein sequences deduced from *AtJAR1* orthologous genes from 71 plant species (Fig. 3). At this point, the separation of AtGH3.10/DFL2-like sequences from the AtJAR1 sequence group was clearly evident and was consistent with the distinction of syntenic sets between the two sequence clades (Fig. 4). Upon verifying the sequence groupings into clades, only 77 protein sequences from 40 plant species representative of the major plant taxa were systematically selected for another round of analysis, from which four major clades were identified: (1) the bryophyte and lycophyte clade, (2) the fern and gymnosperm clade, (3) the angiosperm clade with AtGH3.10-like sequences, and (4) another angiosperm clade with AtJAR1-like sequences (Fig. 5).

Both AtGH3.10- and AtJAR1-like sequences were present in a basal angiosperm species (magnoliid), suggesting that these sequences possibly diverged at the time when flowering plants emerged. Notably, the AtJAR1-like sequences appeared to have diversified across both monocot and eudicot lineages, yet the diversification of AtGH3.10-like sequences seemed to be restricted to eudicots and the sequences remained unduplicated or singly represented in many monocot taxa (Fig. 5). Interestingly, no AtGH3.10-like sequences were found in the grass family

(Poaceae). These findings suggested that AtGH3.10 had a long phylogenetic history of origin rather than just a product of a recent gene duplication event.

2.0 Recombinant AtGH3.10 conjugates JA to isoleucine and other amino acids

To ascertain whether *AtGH3.10* encodes a functional JA-amido synthetase, GST-fused AtGH3.10 and AtJAR1 proteins were expressed in *E. coli* and partially purified the proteins through glutathione-based affinity method (Fig. 6a). The enzymatic activities of the recombinant proteins were measured *in vitro* wherein the reaction products were quantified by LC-MS/MS analysis. Using racemic JA and L-Ile as substrates, both GST-AtGH3.10 and GST-AtJAR1 produced JA-Ile (Fig. 6b,c). Natural isomers of JA-Ile, namely, (+)-*cis*-JA-Ile and (–)-*trans*-JA-Ile, were detected as the major reaction products, while low level of the unnatural form (+)-*trans*-JA-Ile (less than 10% of the natural isomer levels) was also detected in both enzyme-catalyzed reactions (Fig. 6b,c; Fig. 7a). Some kinetic parameters were also estimated to compare the two enzymes. The affinity of GST-AtGH3.10 to JA, as represented by K_m value, was approximately two-fold weaker than that of GST-AtJAR1, whereas both enzymes had comparable affinities to Ile (Table 1, Fig. 7b). Moreover, the specific activity of GST-AtJAR1 was comparable to that of GST-AtGH3.10 in a JA-limited condition, but GST-AtJAR1 had lower specific activity (by about 3-fold) than GST-AtGH3.10 in an Ile-limited condition (Table 1).

Since JA amino acid conjugates other than JA-Ile are also endogenously produced, the activities of recombinant AtGH3.10 and AtJAR1 were compared in the presence of five amino acids whose JA-conjugated forms are reportedly bioactive (Staswick and Tiryaki, 2004; Yan *et al.*, 2016). Under equal and non-limiting concentrations of both JA and the amino acid substrates, GST-AtGH3.10 had conjugating activities for all five amino acids tested that were notably higher than those of GST-AtJAR1 (Fig. 7c). Both GST-AtGH3.10 and GST-AtJAR1 produced JA-Ile at statistically comparable levels. While the amounts of jasmonoyl-alanine (JA-Ala), jasmonoyl-leucine (JA-Leu), jasmonoyl-methionine (JA-Met), and jasmonoyl-valine (JA-Val) produced by GST-AtJAR1 were less than 20% of the highest JA-amido conjugate quantified, the production of JA-amino acid conjugates was remarkably higher for GST-AtGH3.10-catalyzed reactions. Thus, the ability of recombinant AtGH3.10 to synthesize JA-Ile and other JA-amino acid conjugates *in vitro* suggested that AtGH3.10 shares a common biosynthetic function with AtJAR1.

3.0 Role of *AtGH3.10* in wounding response

3.1 Wounding induces *AtGH3.10* expression

After establishing its *in vitro* activity, the physiological functions of *AtGH3.10* were analyzed. Loss-of-function mutants of *AtGH3.10* were generated from wild type (WT, Col-0) and *jar1-11* backgrounds through the CRISPR-Cas9 system (Fig. 8a). A mutant line in WT background was selected which has a 10-base pair deletion in the *AtGH3.10* genomic sequence that consequently caused a frameshift in the coding sequence. In contrast with the 591-amino acid WT AtGH3.10 protein, the frameshift likely resulted in a 137-amino acid truncated protein (Fig. 8b,c). In the *jar1-11* background, a mutant line with a single nucleotide insertion in the *AtGH3.10* coding sequence was obtained, presumably translating a 148-amino acid polypeptide product (Fig. 8b,c). Both mutations were further confirmed by DNA sequencing of *AtGH3.10* transcripts amplified from cDNA of mutant plants (Fig. 8d). The resulting mutants, hereafter referred to as *gh3.10-1* and *gh3.10-2 jar1-11,* respectively, were used for phenotypic analyses.

Since JA signaling plays an essential role in plant responses to physical damage, this study investigated whether *AtGH3.10* responds to wounding as *AtJAR1* does. Four rosette leaves of five-week-old plants were wounded, and the expression of *AtGH3.10* and *AtJAR1* in the wounded leaves was analyzed. Notably, the expression of *AtGH3.10* was not induced by 30 minutes post wounding but was eventually elicited sometime between 30 and 120 minutes, unlike the immediate induction of *AtJAR1* expression 30 minutes after wounding (Fig. 9a). Meanwhile, the expression of both genes was significantly attenuated in their respective mutant states. Transcripts of *AtGH3.10* were still produced in *gh3.10-1* and *gh3.10-2 jar1-11*, although the levels were significantly lower than in WT. This result was expected since the mutations introduced to the *AtGH3.10* genomic sequence were limited to 10 nucleotide positions or less as described above, but these remaining transcripts were likely to translate truncated and dysfunctional proteins (Fig. 8b,c). In contrast, the presence of *AtJAR1* transcripts was nearly abolished in the *jar1-11* background, which might have been due to the insertion of a T-DNA fragment in the gene's genomic region (https://www.arabidopsis.org/).

The involvement of *AtGH3.10* in wound responses was ascertained by the expression of two wound-inducible, JA-responsive genes. The expression of *OPR3*, which encodes an enzyme required for JA biosynthesis, was substantially induced to comparable levels in WT, *gh3.10-1*, and *jar1-11* by 30 minutes after wounding but was only minimally induced in *gh3.10-2 jar1-11* (Fig. 9b). At 120 minutes following wounding, the expression of *OPR3* had already declined significantly, especially in WT, *gh3.10-1*, and *jar1-11*. *JAZ1* had a similar expression pattern as *OPR3*. *JAZ1* was highly induced in WT, *gh3.10-1*, and *jar1-11* 30 minutes following wounding but was only minimally induced in *gh3.10-2 jar1-11* (Fig. 9b). At 120 minutes post wounding, the *JAZ1* levels in WT and single mutants tended to decrease. Taken together, these results demonstrated that the expression of *AtGH3.10* was wound-inducible and that its activity alone was sufficient to elicit the wound-inducible expression of *OPR3* and *JAZ1* that otherwise barely occurred in *gh3.10-2 jar1-11*.

3.2 *AtGH3.10* contributes to the JA-amino acid pool in the leaves

The endogenous levels of JA and JA-amino acid conjugates in rosette leaves were quantified (Fig. 10) to further explore the function of *AtGH3.10* in wound response. Substantial accumulation of JA occurred in the wounded leaves of all genotypes by 30 minutes as compared to their respective unwounded levels (Fig. 11). JA-Ile accumulated similarly in the leaves of both WT and *gh3.10-1* 30 minutes after wounding, at levels that were over 200-fold higher than the basal (unwounded) levels (Fig. 11). In *jar1-11* leaves, slight increase in JA-Ile level occurred by 30 minutes after wounding but the level was less than 5% of that in WT at the same time point. While there was no JA-Ile detected in the unwounded leaves of *gh3.10-2 jar1-11*, trace amounts of the hormone were still detected at 30 and 120 minutes after wounding. By 120 minutes, the amount of JA-Ile eventually decreased by about 76% in WT, *gh3.10-1*, and *jar1-11* (Fig. 11).

To understand how the wound responses of *jar1-11* and *gh3.10-2 jar1-11* differed despite the seeming little difference in their JA-Ile levels, the catabolic form of JA-Ile (the 12OH-JA-Ile) and the other bioactive JA-amino acid conjugates were also analyzed. Concurrent with the eventual decline of JA-Ile level by 120 minutes post wounding, the level of 12OH-JA-Ile increased dramatically through time (Fig. 11). The wounded leaves of *jar1-11* accumulated 12OH-JA-Ile by over 300-fold greater than did *gh3.10-2 jar1-11* at 120 minutes post wounding. Moreover, the 12OH-JA-Ile level was lower by about 30% in *gh3.10-1* than that in WT, hence implying the contribution of *AtGH3.10* to the hormone pool. The catabolite, however, was not detected in unwounded *gh3.10-2 jar1-11* and only minuscule amount below the limit of quantitation were recorded 30 minutes after wounding (Fig. 11). Meanwhile, some increases in the levels of JA-Ala were observed upon wounding for WT and single mutants, while significant wound-induced accumulations in JA-Val were noted only in WT and *gh3.10-1* (Fig. 12). Relative to JA-Ile, the levels of JA-Ala and JA-Val were substantially lower in the leaves even after wounding. JA-Met and JA-Leu, on the other hand, could not be quantified. Considering the hormone level differences across genotypes especially those of JA-Ile and 12OH-JA-Ile, the contribution of *AtGH3.10* in the biosynthesis of jasmonates during wound stress response in Arabidopsis was revealed.

3.3 Systemic induction of *AtGH3.10* upon wounding

Aside from local induction of jasmonate accumulation by wounding, indications of a systemic response have been reported (Glauser *et al.*, 2008; Koo *et al.*, 2009). The involvement of *AtGH3.10* in this response was also investigated. From a separate batch of plants, four rosette leaves of each plant were wounded. The wounded leaves and the unwounded ones in between them were collected 120 minutes after wounding. *AtGH3.10* was expressed significantly higher in the rosette leaves of *jar1-11* plants that experienced distal wounding (hereafter referred to as systemic leaves) than in the leaves of unwounded *jar1-11* plants (Fig. 13a). In contrast, the induction of *AtJAR1* expression was not observed in the systemic leaves and instead the transcript decreased in *gh3.10-1* (Fig. 13a). Concurrently, JA levels significantly increased in the systemic leaves of WT, *gh3.10-1*, *jar1-11*, and *gh3.10-*

2 jar1-11 compared to their basal levels in unwounded plants (Fig. 13b). Comparing the JA levels between the unwounded and the systemic leaves of WT, the magnitude of the effect size was categorically large (Cohen's d = 1.39), thus confirming the systemic nature of the jasmonate response to wounding. Additionally, the levels of JA-Ile concomitantly increased in the systemic leaves of *gh3.10-1*, *jar1-11*, and *gh3.10-2 jar1-11* relative to the levels in their corresponding unwounded leaves. Despite the statistical insignificance of the difference in JA-Ile levels between the unwounded and the systemic leaves of WT (Fig. 13b), the effect size was still large (Cohen's d = 1.33), implying that the JA-Ile level was higher in the systemic leaves than in the unwounded leaves by as much as 2.19 pg/mg fresh weight (FW). The observed systemic induction of *AtGH3.10* expression was further supported by the detection of *AtGH3.10*-promoter activity in the unwounded leaves that were situated adjacent to the wounded ones after GUS staining (Fig. 14). These results suggested that the expression of *AtGH3.10* and the respective production of bioactive JAs could be elicited systemically under wound stress, at least when *AtJAR1* was inoperative.

4.0 Role of *AtGH3.10* in flower development

4.1 *AtGH3.10* functions with *AtJAR1* in maintaining stamen development

Since jasmonates are indisputable regulators of plant growth and flower development (Creelman and Mullet, 1997; Wasternack and Hause, 2013), morphological assessment of the mutants was performed. The inflorescences of *gh3.10-2 jar1-11* were notably longer than those of WT and single mutants 42 days after germination (Fig. 15; Fig. 16a,b). The inflorescences of WT, *gh3.10-1*, and *jar1-11* had no remarkable differences by visual inspection but a higher number of flowers at anthesis and later stages, characterized by visible petals, was observed in *gh3.10-2 jar1-11* (Fig. 17a,b). This anomaly likely indicates a delay or failure in the progression of flower maturation process from blossoming to silique formation. To substantiate this observation, at least 21 flowers at developmental stage 14 (Smyth *et al.*, 1990) were collected from each genotype and dissected. Shorter stamen filaments were observed in about half of the number of flowers examined from *gh3.10-2 jar1-11* and only a few in *jar1-11* but not in WT and *gh3.10-1* flowers whose stamen filaments were long enough for the anthers to touch the stigma (Fig. 18a). Furthermore, the anther dehiscence in *gh3.10-2 jar1-11* was notably reduced, as anthers dehisced mildly (29%) or not at all (33%) (Fig. 18a). These phenotypes were consistent with a higher proportion of undeveloped siliques observed in *gh3.10-2 jar1-11* compared to the other genotypes (Fig. 18b,c). "Undeveloped" silique was defined in this study as the one being immature, obviously dwarfed, and devoid of seeds.

The genetic basis of *gh3.10-2 jar1-11* flower phenotype was explored further. Comparative qPCR analysis of *AtGH3.10* and *AtJAR1* expression in the flower buds showed that the level of *AtGH3.10* transcripts was lower in *jar1-11*; similarly, the transcript of *AtJAR1* was reduced in *gh3.10-1* relative to their respective WT levels (Fig. 19a). This suggested that, in flower, the expression of *AtGH3.10* affects that of *AtJAR1* and *vice versa*. To further show the involvement of *AtGH3.10* in flower development, a promoter-reporter assay was performed by introducing a *AtGH3.10promoter::GUS* (β-glucuronidase) construct into WT and *jar1-11* plants. Under normal conditions, the GUS staining was observed in the flower buds and young siliques of WT and *jar1-11* (Fig. 19b), suggesting the localized expression of *AtGH3.10* in those tissues. This localization pattern of promoter activity is similar to that of *AtJAR1* as previously demonstrated (Chen *et al.*, 2007).

4.2 *AtGH3.10* contributes to the jasmonate pool in flowers

To determine the effects of the mutations on the hormone levels in plants, quantitative LC-MS/MS analysis of endogenous JA and JA-amino acid conjugates was carried out. Flower buds at stage 12 and earlier stages were excised from the pedicels and analyzed. The JA level was significantly higher in *jar1-11* and *gh3.10-2 jar1-11* compared to WT, but it was lower in *gh3.10-1* (Fig. 20). On the other hand, the JA-Ile level was lower in *gh3.10-1* than in WT (Fig. 20). JA-Ile was appreciably lower in the flower buds of *jar1-11* compared to those of WT and *gh3.10-1*. Interestingly, a residual amount of the hormone persisted in the flower buds of *gh3.10-2 jar1-11*. Since the level of JA-Ile in *jar1-11* is relatively low, it was verified whether much of the hormone was catabolized to its hydroxylated form. The level of 12OH-JA-Ile was about 40% lower in the flower buds of *gh3.10-1* compared to the WT level, highlighting the contribution of *AtGH3.10* in JA-Ile production and subsequent 12OH-JA-Ile accumulation (Fig. 20). In *jar1-11*, the level of 12OH-JA-Ile in the flower buds was about 80% less relative to WT. Notably, no 12OH-JA-Ile was detected in the floral tissues of *gh3.10-2 jar1-11*. Four JA-amino acid conjugates with reported bioactivity were also quantified. JA-Ala and JA-Val were detected but JA-Leu and JA-Met could not be quantified (Fig. 20). Only minimal differences were evident across genotypes for JA-Ala but those for JA-Val, which could promote COI1-JAZ interaction *in vitro* better than JA-Ala or JA-Met (Katsir *et al.*, 2008), were considerable. JA-Val level was lower in *gh3.10-1* than in WT and was significantly less in *jar1-11* and *gh3.10-2 jar1-11* (Fig. 20). So far, the collective results of morphological and physiological analyses suggested that *AtGH3.10* contributes to the maintenance of normal flower development in Arabidopsis.

4.3 The effect of *AtGH3.10* in flower development is JA-mediated

To confirm whether the flower phenotype observed in *gh3.10-2 jar1-11* was JA signaling-mediated, the *JAZ1* expression, a known JA-responsive marker gene and a transcriptional repressor of JA-response genes, was analyzed. Significant downregulation of *JAZ1* expression with large effect size (Cohen's d = 3.03) was observed in the flower buds of *gh3.10-2 jar1-11* (Fig. 21a). To see how this altered *JAZ1* expression affected downstream signaling, the expression of two JA-responsive transcription factors, *MYB21* and *MYB24*, was analyzed. Both transcription factors ensure normal stamen development in Arabidopsis and are direct targets of *JAZ1* (Song *et al.*, 2011). The expression of *MYB21*, whose role in stamen development is dominant over *MYB24* (Mandaokar *et al.*, 2006), was significantly abated in *gh3.10-2 jar1-11* (Cohen's d = 2.77) but not in *jar1-11* nor in *gh3.10-1* single mutant (Fig. 21b). No significant change in *MYB24* expression was observed. Based on this flower development-related gene expression and on the observed floral morphology especially in *jar1-11*, the level of bioactive jasmonate that *AtGH3.10* produces in the plant was sufficient to maintain the normal flower development and silique formation to a considerable extent in the absence of *AtJAR1*.

5.0 Responses of *AtGH3.10-JAR1* mutants to exogenous JA and red light

The sensitivity of root growth to inhibition by JA was assessed. WT and mutant plants were germinated and grown on agarose nutrient medium containing 5 µM JA for 14 days. Both the *jar1-11* and *gh3.10-2 jar1-11* (15.6 mm and 20.38 mm average lengths, respectively) plants exhibited longer roots and hence were comparatively less sensitive to JA than were WT and *gh3.10-1* plants (4.0 mm and 6.6 mm, respectively) (Fig. 22a,b).

Since previous overexpression and antisense tuning of *AtGH3.10* in Arabidopsis showed light-dependent regulation of hypocotyl elongation (Takase *et al.*, 2003), the growth of *gh3.10-1* under light exposure was tested. Seeds were germinated and allowed to grow for 5 days under continuous red light with fluence rate of 5 µmol m^{-2} s^{-1}. Significant hypocotyl elongation was observed in *jar1-11* and *gh3.10-2 jar1-11* seedlings compared with WT (Fig. 23). The *gh3.10-1* seedlings likewise showed significant hypocotyl elongation relative to WT. Although the average hypocotyls of *jar1-11* were markedly longer than those of WT and *gh3.10-1*, it was noteworthy that the top 50 percent of the measured lengths in *gh3.10-1* was comparable with nearly all measurements obtained in *jar1-11* (Fig. 23). This may suggest that *AtGH3.10* had arguably substantial share of function with *AtJAR1* in the context of light-dependent modulation of hypocotyl growth.

TABLE

Table 1. Kinetic parameters of recombinant AtGH3.10 and AtJAR1

Enzyme	Substrate	K_M (μM)	Specific activity (μM/min/mg protein)
GST-AtGH3.10	JA	148.2 ± 35.3	92.4 ± 28.8
	Ile	81.5 ± 30.3	91.6 ± 25.0
GST-AtJAR1	JA	65.5 ± 7.3	105.9 ± 17.4
	Ile	81.4 ± 11.6	34.7 ± 4.4

Values are the means of four experiments ± SEM

FIGURES

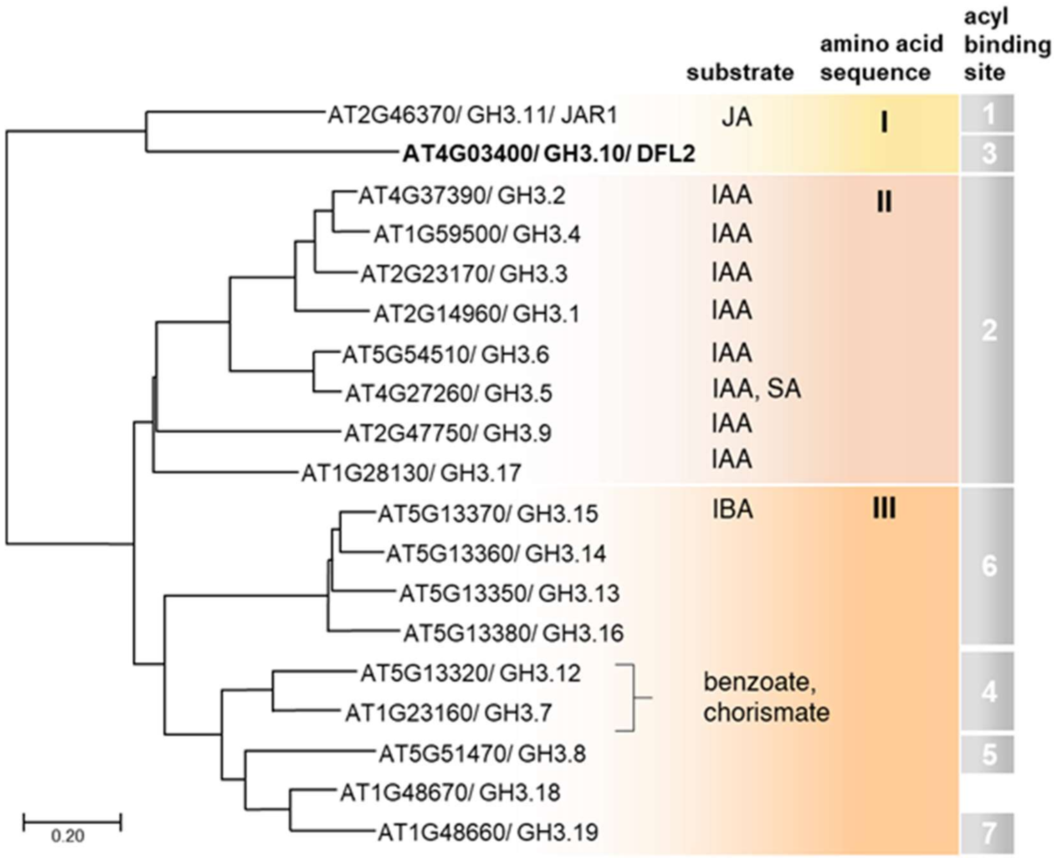

Figure 2. Phylogeny of GH3 protein family in Arabidopsis

Members of the Arabidopsis GH3 protein family were grouped based on their known substrate/s, their amino acid sequences, and the sequences of their acyl acid-binding sites as shown by Westfall *et al.* (2012). The Neighbor-Joining phylogenetic tree was inferred from 19 protein sequences. The scale indicates the evolutionary distance in number of amino acid substitutions per site unit and was computed using the JTT matrix-based method with gamma distribution to model rate variation among sites. JA, jasmonic acid; IAA, indole-3-acetic acid; IBA, indole-3-butyric acid.

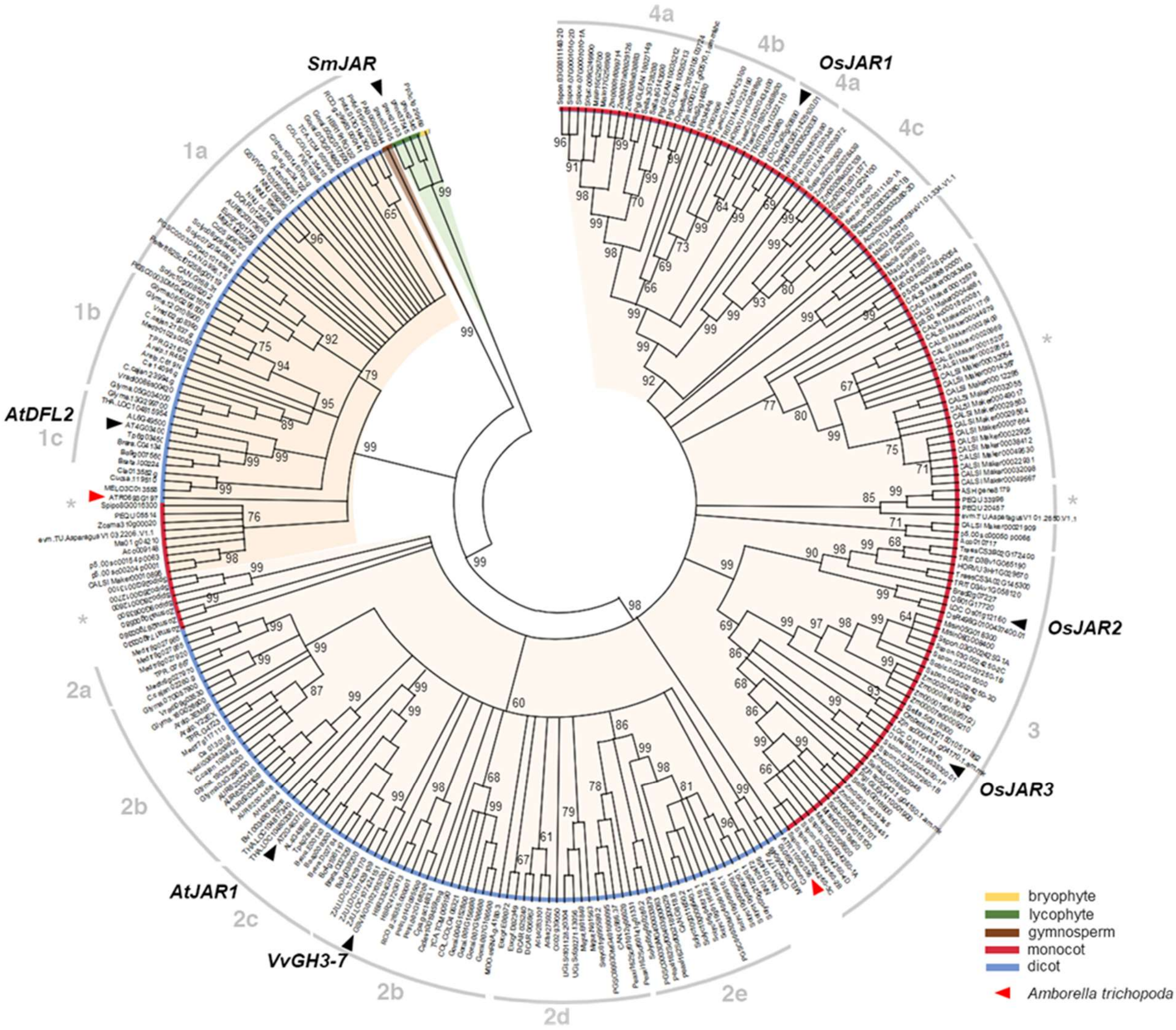

Figure 3. Evolutionary history of Group I GH3 gene family in plants

Maximum likelihood-based phylogenetic tree of 287 protein sequences deduced from *AtJAR1* orthologous genes from 71 plant species. Numbers at nodes represent bootstrap support values from 500 replications, where branches with less than 60% values were collapsed. JAR1 genes previously characterized were shown (*SmJAR1*, *Selaginella moellendorffii*; *AtDFL2*/*GH3.10* and *AtJAR1*, *A. thaliana*; *VvGH3-7*, *Vitis vinifera*; *OsJAR1,2,3*, *Oryza sativa*). Numbers with letters in grey indicate syntenic sets based on syntenic orthologs (Figure 2). Asterisks indicate clades with unassigned syntenic grouping due to high divergence, lack of information, or limited genomic region coverage.

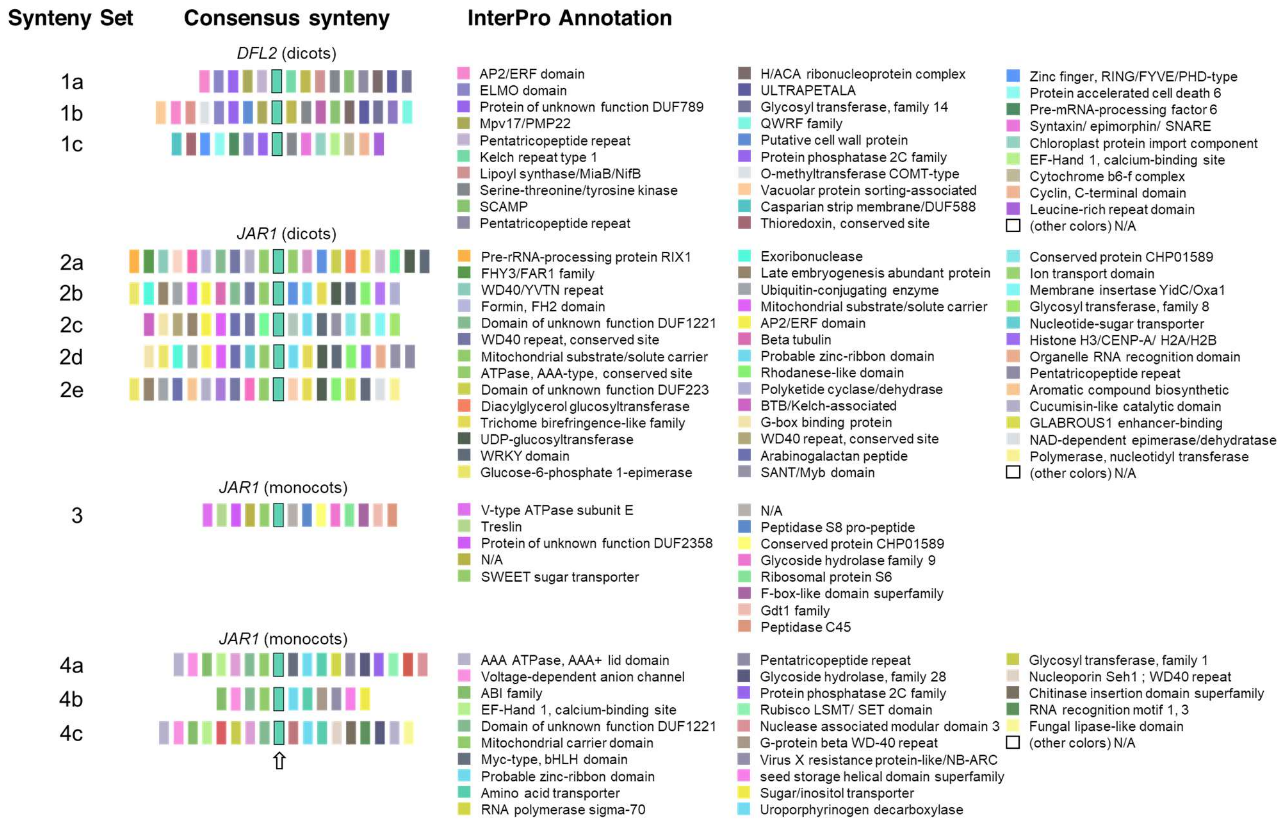

Figure 4. Syntenic sets of plant Group I GH3 orthologous genes and their corresponding consensus synteny plot

A syntenic set was identified based on the similarity in gene composition among genomic regions, each region consisted of 30 neighboring genes flanking the *JAR1* or *GH3.10* gene (arrow). A consensus synteny plot represents the prevailing gene composition (and essentially gene order) of a synteny set, wherein each colored box is a gene that occur more than 60% of the time among the genomic regions belonging in a particular syntenic set. Each color indicates a homologous gene family with its InterPro annotation given.

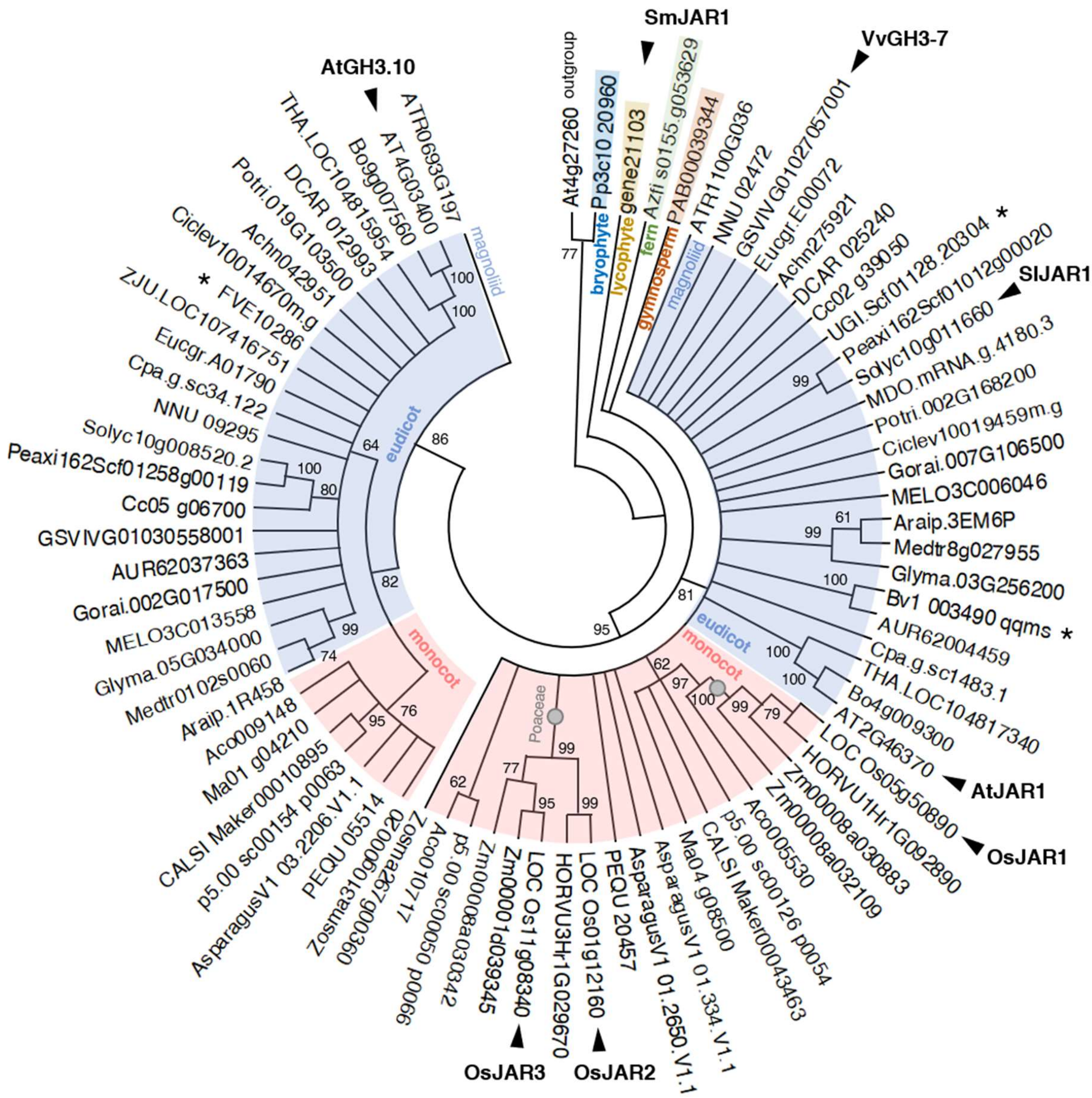

Figure 5. Phylogeny of representative plant GH3 proteins

Maximum likelihood-based phylogeny of 77 protein sequences deduced from *AtJAR1* orthologous genes from 40 species representing the major taxonomic groups of plants. The tree was a consensus inferred from 1000 bootstrap replications. Bootstrap support values higher than 60 are shown at each node. Previously characterized AtJAR1 orthologs are indicated (SmJAR1, *Selaginella moellendorffii*; AtGH3.10 and AtJAR1, *A. thaliana*; VvGH3-7, *Vitis vinifera*; SlJAR1, *Solanum lycopersicum*; OsJAR1,2,3, *Oryza sativa*). Asterisks indicate sequences that have no AtGH3.10 or AtJAR1 counterpart. Outgroup is AtGH3.5.

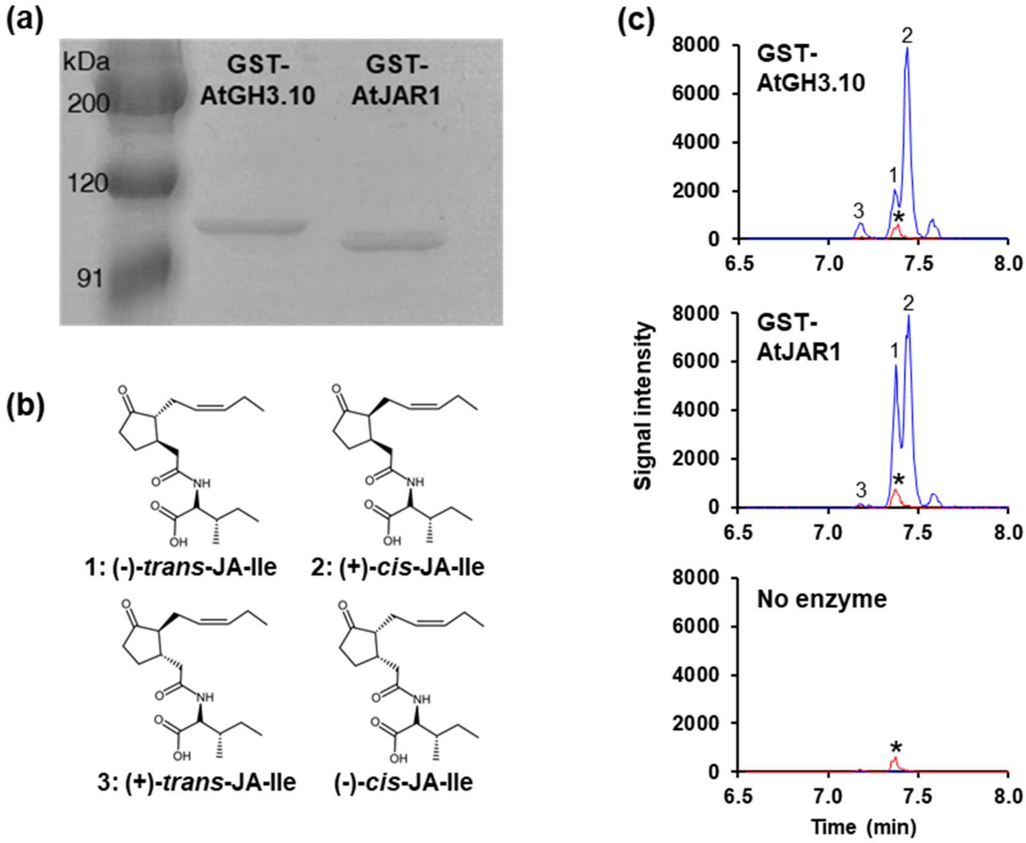

Figure 6. Enzymatic activity of recombinant AtGH3.10 and AtJAR1

(a) GST-AtGH3.10 and GST-AtJAR1 recombinant proteins (500 ng each) on SDS-PAGE gel after affinity purification and filter concentration. (b) Chemical structures of JA-Ile isomers. (c) LC-MS/MS chromatograms of JA-Ile isomers detected in enzyme activity assays of GST-AtGH3.10 and GST-AtJAR1. The blue and red lines indicate mass chromatograms of JA-Ile and JA-[$^{13}C_6$]Ile, respectively. Asterisk indicates the peak for (–)-*trans*-JA-L-[$^{13}C_6$]Ile. Numbers 1, 2, and 3 indicate the peaks of (–)-*trans*-JA-L-Ile, (+)-*cis*-JA-L-Ile, and (+)-*trans*-JA-L-Ile, respectively.

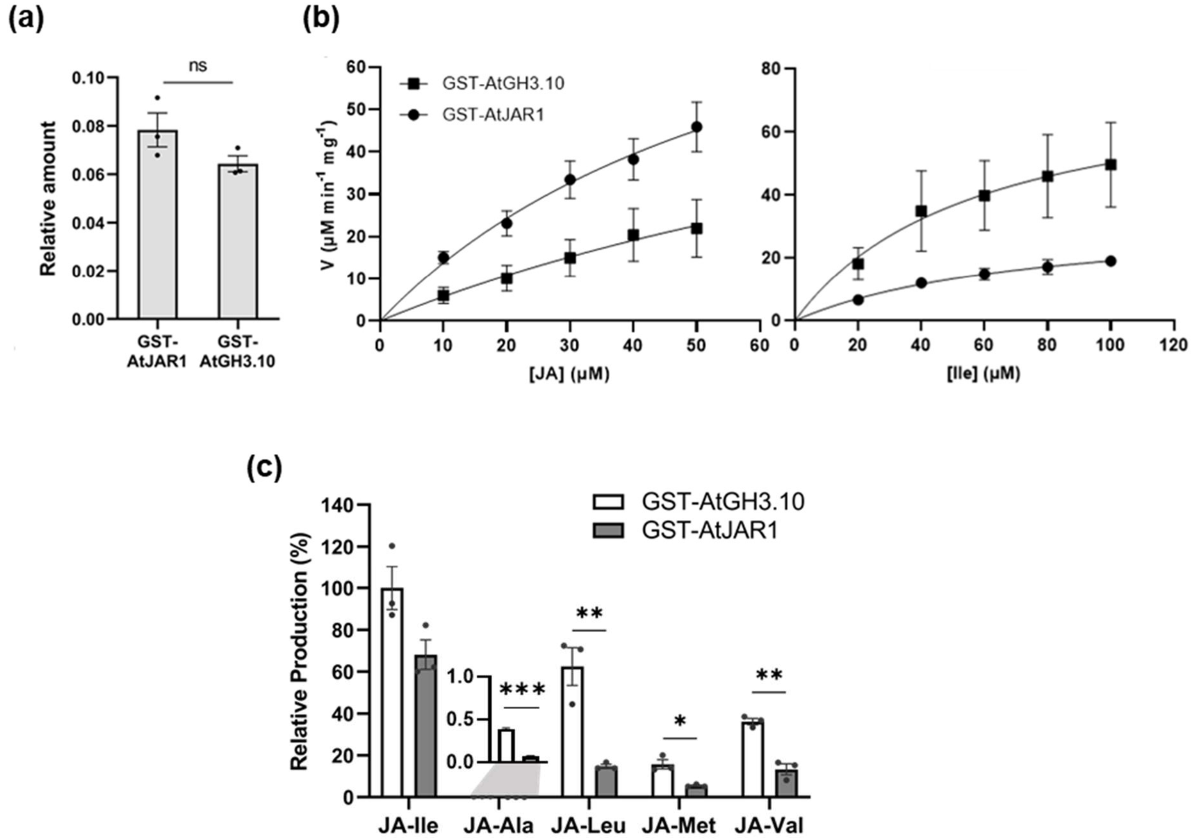

Figure 7. Enzyme activity and kinetics of recombinant AtGH3.10 and AtJAR1

(a) Amount of unnatural JA-Ile isomers detected relative to natural isomers. ns means not significantly different by Student's *t*-test. (b) Michaelis-Menten plots of enzymatic activities of GST-AtGH3.10 and GST-AtJAR1 with varying concentrations of (–)-JA or Ile. Each point represents the mean ± the SEM of four independent experiments. (c) Relative production of JA-isoleucine (JA-Ile), JA-alanine (JA-Ala), JA-leucine (JA-Leu), JA-methionine (JA-Met), and JA-valine (JA-Val) by GST-AtGH3.10 and GST-AtJAR1. The JA-amino acid products were quantified by LC-MS/MS from a reaction mixture containing 1 mM JA, 1 mM amino acid, and 2 pmol enzyme and are expressed as percentage relative to the highest product detected. Bars represent the mean from three independent experiments ± SEM. Asterisks indicate significant differences by Student's *t*-test (**p*<0.05, ***p*<0.01, ****p*<0.0001).

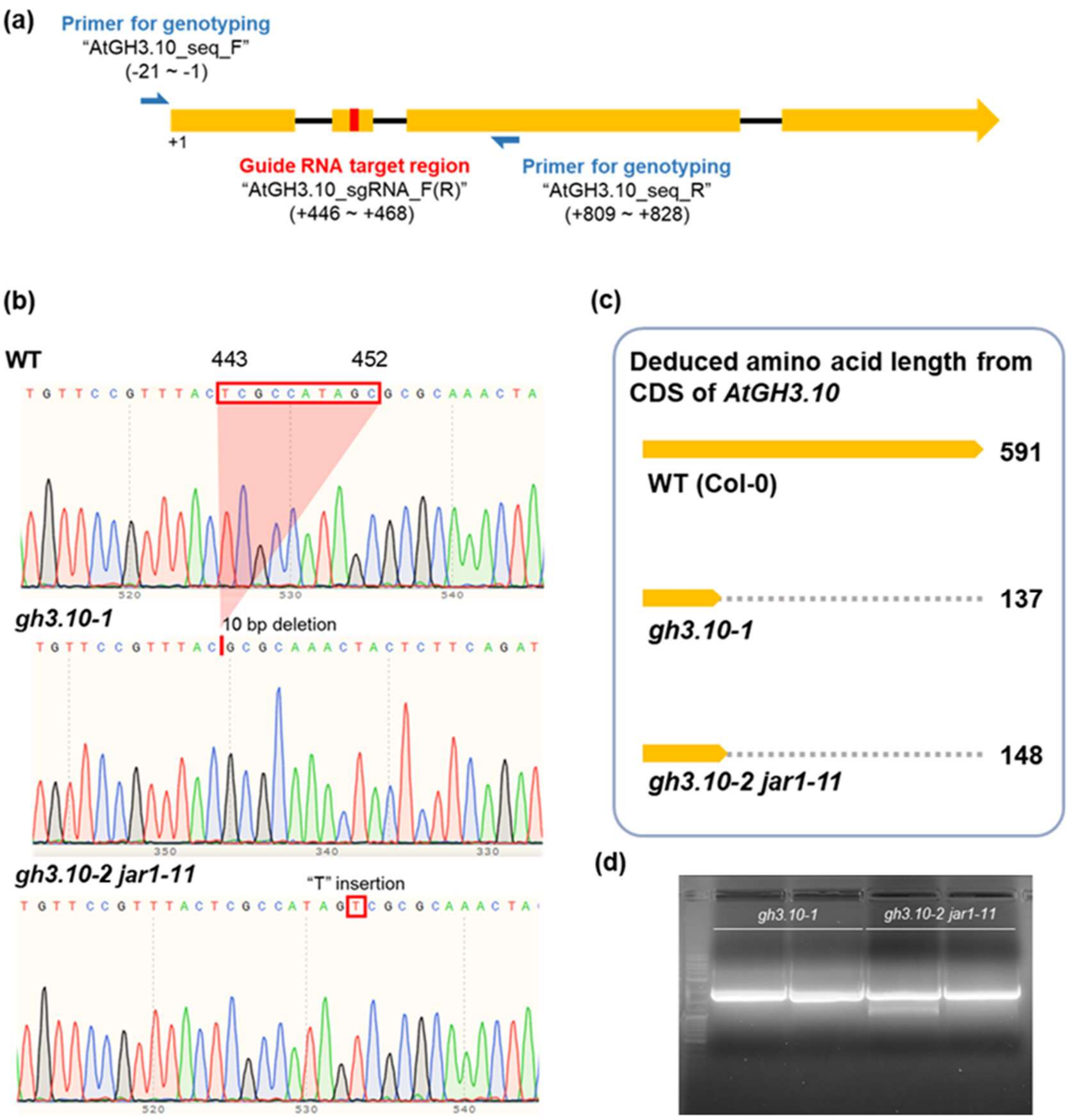

Figure 8. Mutations in *AtGH3.10* sequence by the CRISPR-Cas9 system

(a) Open reading frame of *AtGH3.10*. Broken yellow arrow indicates exons; black lines indicate introns. The guide RNA target region is shown by red box, and primer sites used for genotyping are indicated by blue arrowheads. The start of coding sequence is indicated by '+1'. (b) Genomic DNA sequences of *AtGH3.10* segments showing the mutations. Images were generated using SnapGene Viewer. (c) Deduced amino acid lengths of translated polypeptides in mutant plants as consequences of mutations. (d) Full CDS transcripts of *AtGH3.10* amplified by PCR from cDNA of *gh3.10-1* and *gh3.10-2 jar1-11* plants. The bands were sequenced and confirmed to have the mutations that were identical to the corresponding mutated genomic sequences shown in (b). The lower band in the third lane was non-specific amplification based on sequence analysis. Two plants per genotype were used for DNA sequencing.

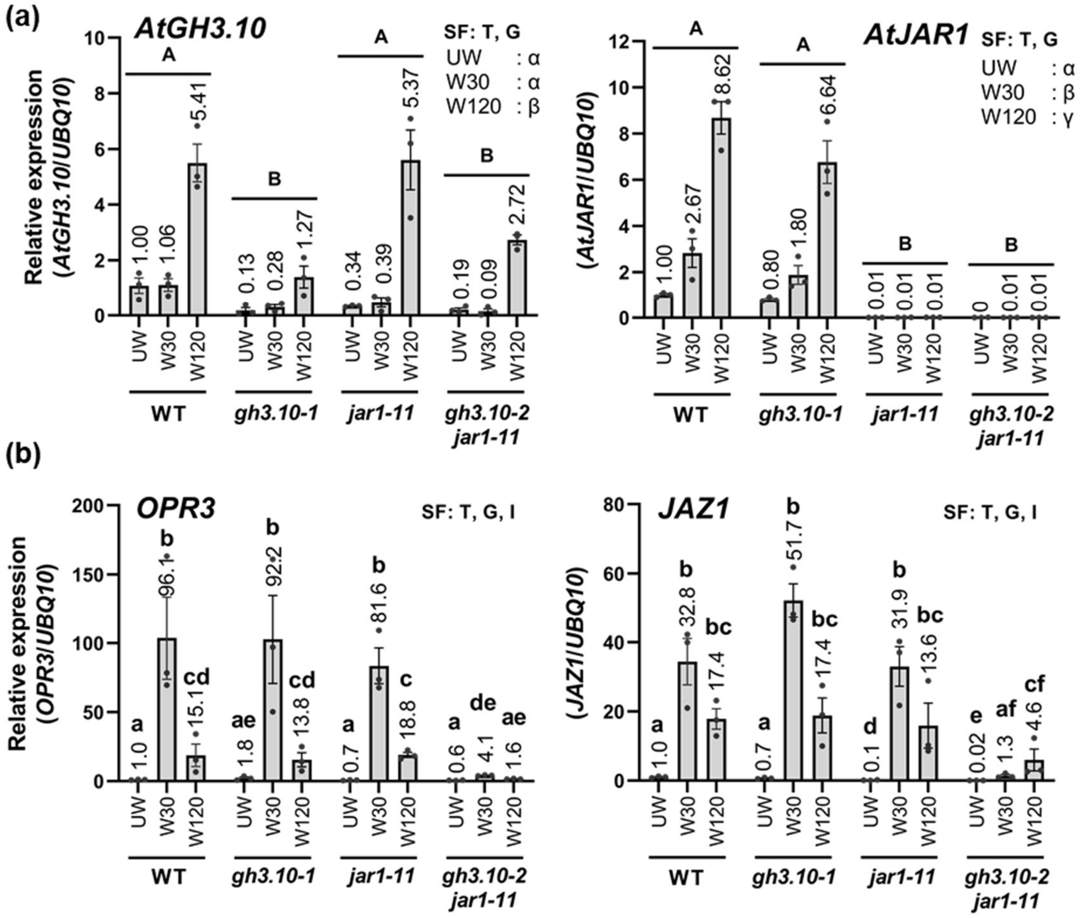

Figure 9. Expression of *AtGH3.10*, *AtJAR1*, and JA-responsive genes upon wounding

(a) Relative expression of *AtGH3.10* and *AtJAR1* in the rosette leaves of unwounded (UW) and wounded 5-week-old plants. Wounded rosette leaves were analyzed at 30 or 120 minutes post wounding (W30 and W120, respectively). **(b)** Wound-induced expression of *OPR3*, a JA biosynthetic gene, and *JAZ1*, a signaling repressor, in rosette leaves of WT and mutant plants. For A and B, expression levels are fold differences relative to WT (UW). Each value represents the mean of three biological replicates with error bars indicating SEM. Significant factors (SF) indicate which of the two independent factors (treatment, T and genotype, G) and/or their interaction (I) are statistically significant by a two-way ANOVA (p<0.05). Significant differences among genotypes, treatments, and genotype-treatment values are indicated by different uppercase letters, Greek letters, or lowercase letters, respectively. All multiple comparisons were evaluated using Tukey's test. *P* values are shown in Method Table 3.

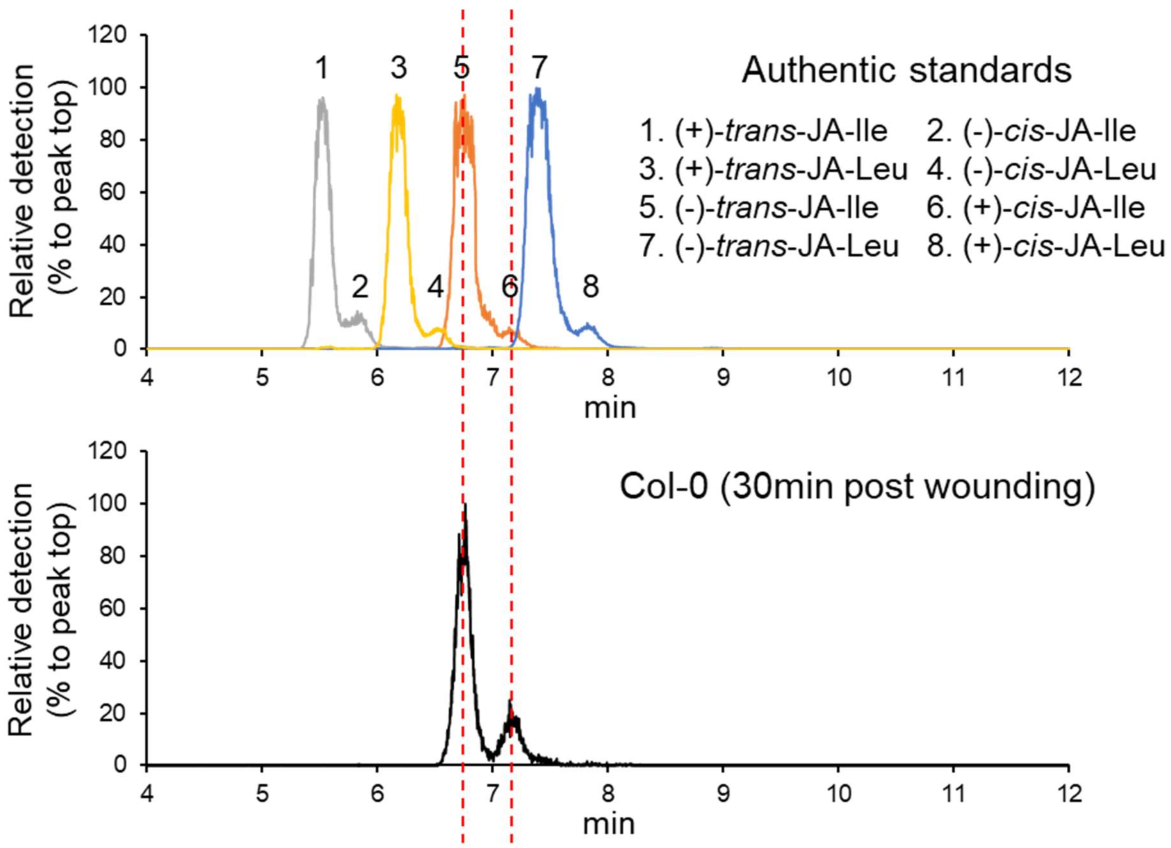

Figure 10. Peak identification of JA-Ile and JA-Leu extracted from plant tissues

Peak identification of JA-Ile and JA-Leu extracted from plant tissues. Detailed LC-MS/MS conditions are shown in Method Table 2 (HPLC method #4). The top chromatogram shows merged chromatograms of authentic standard mixtures: (+)-*trans*-JA-Ile and (–)-*cis*-JA-Ile (gray, peak 1 & 2), (+)-*trans*-JA-Leu and (–)-*cis*-JA-Leu (yellow, peak 3 & 4), (–)-*trans*-JA-Ile and (+)-*cis*-JA-Ile (orange, peak 5 & 6), (–)-*trans*-JA-Leu and (+)-*cis*-JA-Leu (blue, peak 7 & 8). The bottom chromatogram shows JA-Ile detection from the extract of Col-0 leaves that were wounded 30 minutes prior to harvesting.

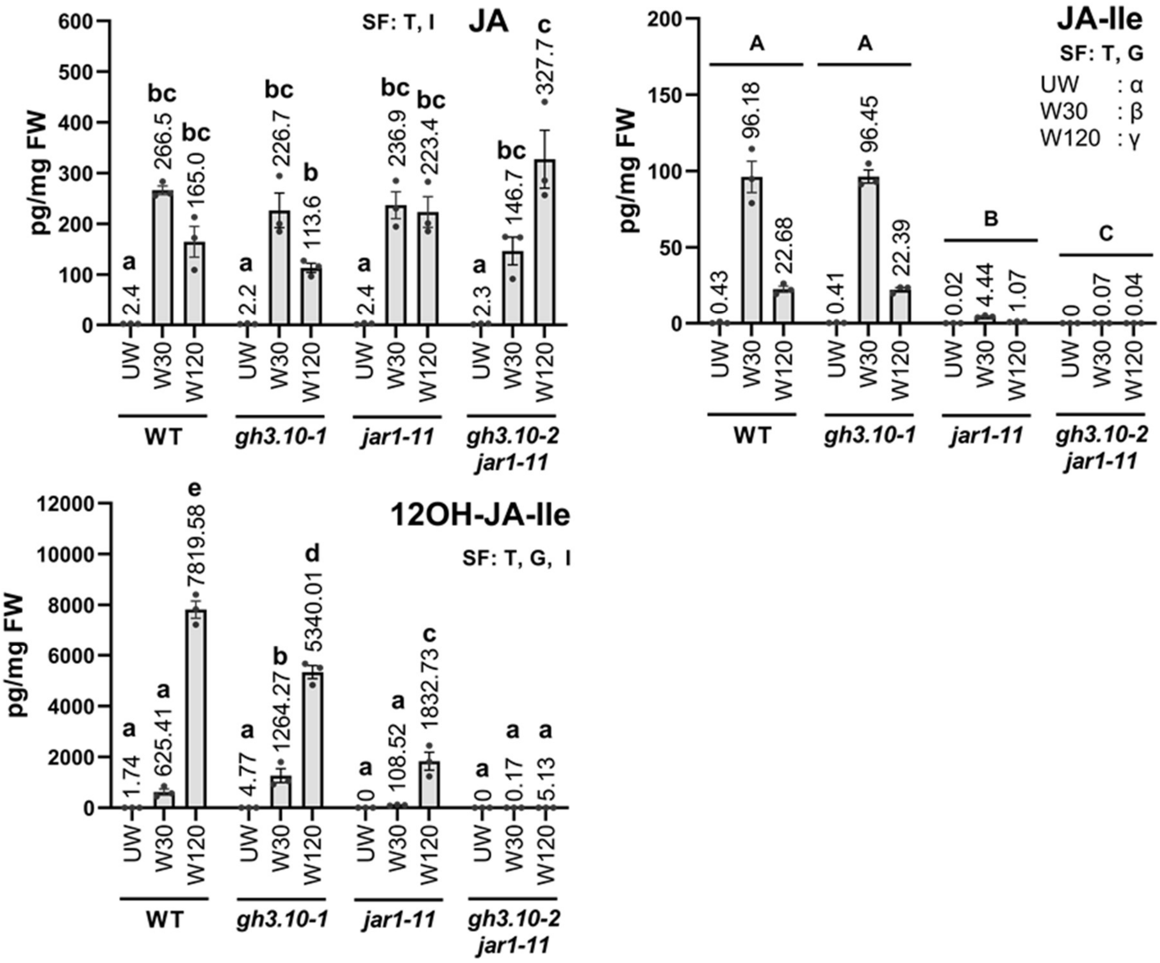

Figure 11. Accumulation of JA and JA-Ile upon wounding

Endogenous levels of JA, JA-Ile, and 12OH-JA-Ile in the leaves under normal and wound stress conditions. Hormones were extracted from either unwounded (UW) or wounded rosette leaves of 5-week-old plants; the latter harvested 30 or 120 mins after wounding (W30 and W120, respectively). Each value represents the average amount from three individual plants ± SEM. Significant factors (SF) indicate which of the two independent factors (treatment, T and genotype, G) and/or their interaction (I) are statistically significant by a two-way ANOVA (p<0.05). Significant differences among genotypes, treatments, and genotype-treatment values are indicated by different uppercase letters, Greek letters, or lowercase letters, respectively. All multiple comparisons were evaluated using Tukey's test. P values are shown in Method Table 3. Note that data on 12OH-JA-Ile was derived from separate batch of plants as those on JA and JA-Ile. LOQ (in pg/mg FW, based on minimum plant weight used): 0.03 (JA), 0.01 (JA-Ile), 0.20 (12OH-JA-Ile).

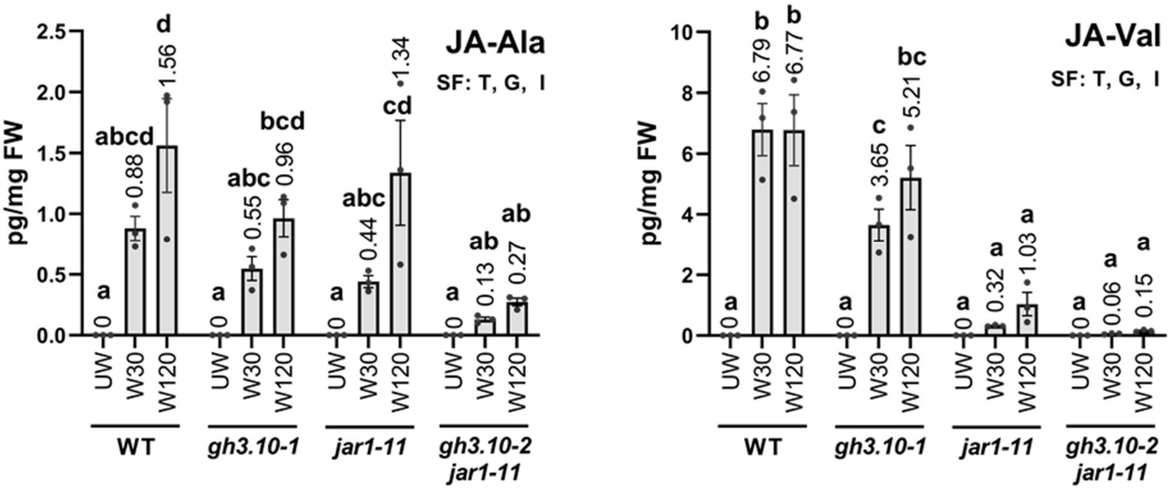

Figure 12. Accumulation of JA-amino acid conjugates upon wounding

Endogenous levels of JA-amido conjugates in the leaves under normal and wound stress conditions. Hormones were extracted from either unwounded (UW) or wounded rosette leaves of 5-week-old plants; the latter harvested 30 or 120 mins after wounding (W30 and W120, respectively). Each value represents the average amount from three individual plants ± SEM. Significant factors (SF) indicate which of the two independent factors (treatment, T and genotype, G) and/or their interaction (I) are statistically significant by a two-way ANOVA (p<0.05). Different lowercase letters indicate significant differences among genotype-treatment values based on Tukey's test. *P* values are shown in Method Table 3. LOQ (in pg/mg FW, based on minimum plant weight used): 0.02 (JA-Ala and JA-Val).

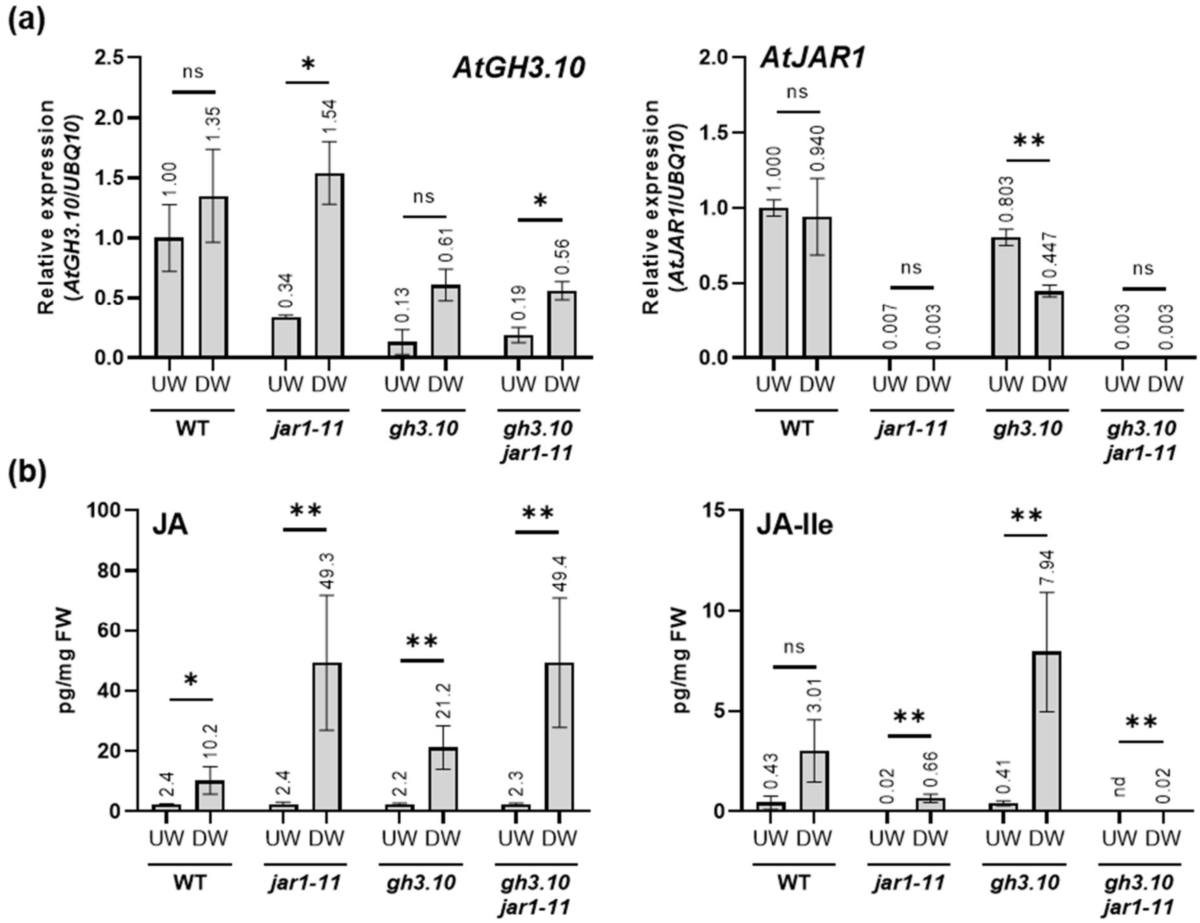

Figure 13. Wound-induced systemic expression of *AtGH3.10* and *AtJAR1* and accumulation of JAs

(a) Relative expression of *AtGH3.10* and *AtJAR1* in rosette leaves of unwounded plants (UW) compared to those in unwounded rosette leaves of wounded plants (distally wounded, DW) 120 mins post wounding. Bars indicate means of three biological replicates ± SEM. Values represent fold change difference from the unwounded WT, which was standardized to *UBQ10* levels. (b) Levels of endogenous JA and JA-Ile. Values are means of three biological replicates ± SEM. Asterisks indicate statistical difference between pairs by Student's t-test (**p*<0.05, ***p*<0.01); ns means not significant.

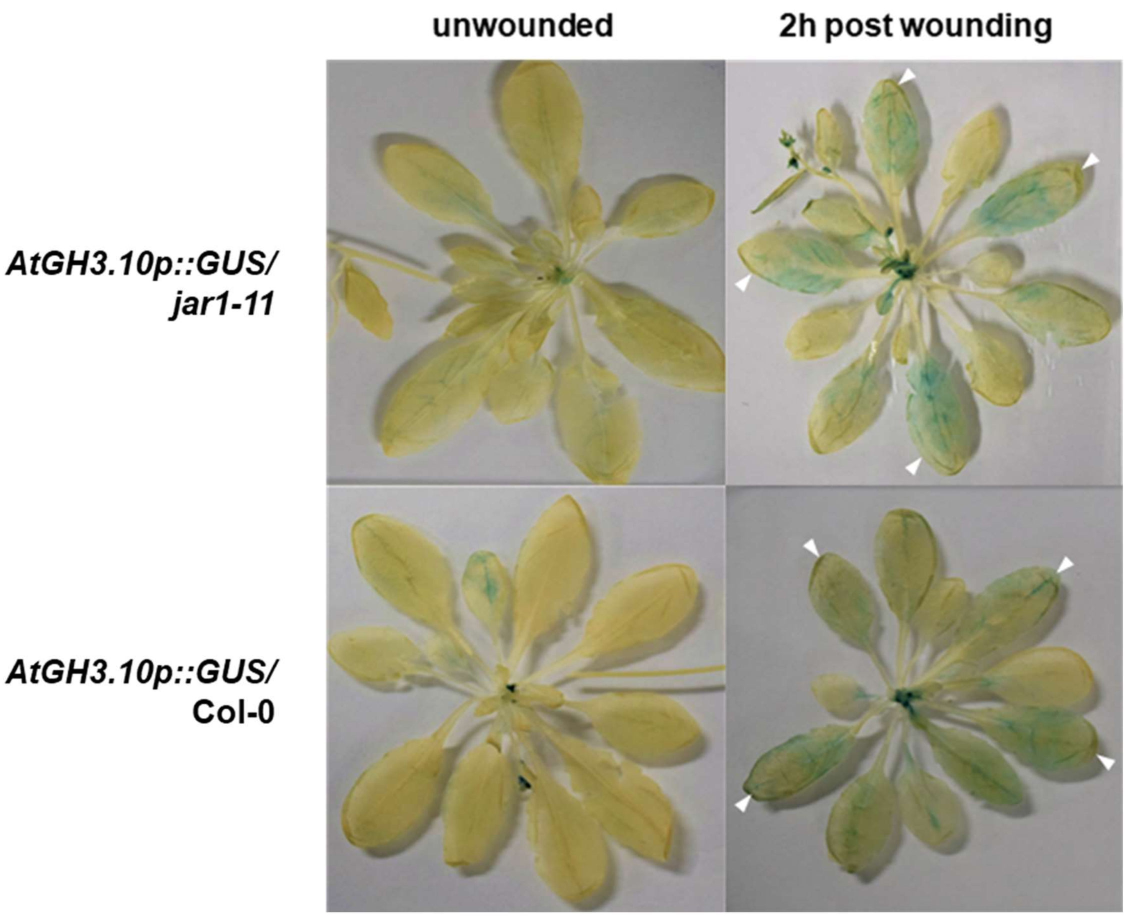

Figure 14. *AtGH3.10* promoter activity upon wounding

Promoter activity of *AtGH3.10* in *jar1-11* and Col-0 plants under normal and wound stress conditions. Plants harboring the *AtGH3.10p::GUS* construct were stained for GUS activity. White arrowheads point the four wounded leaves.

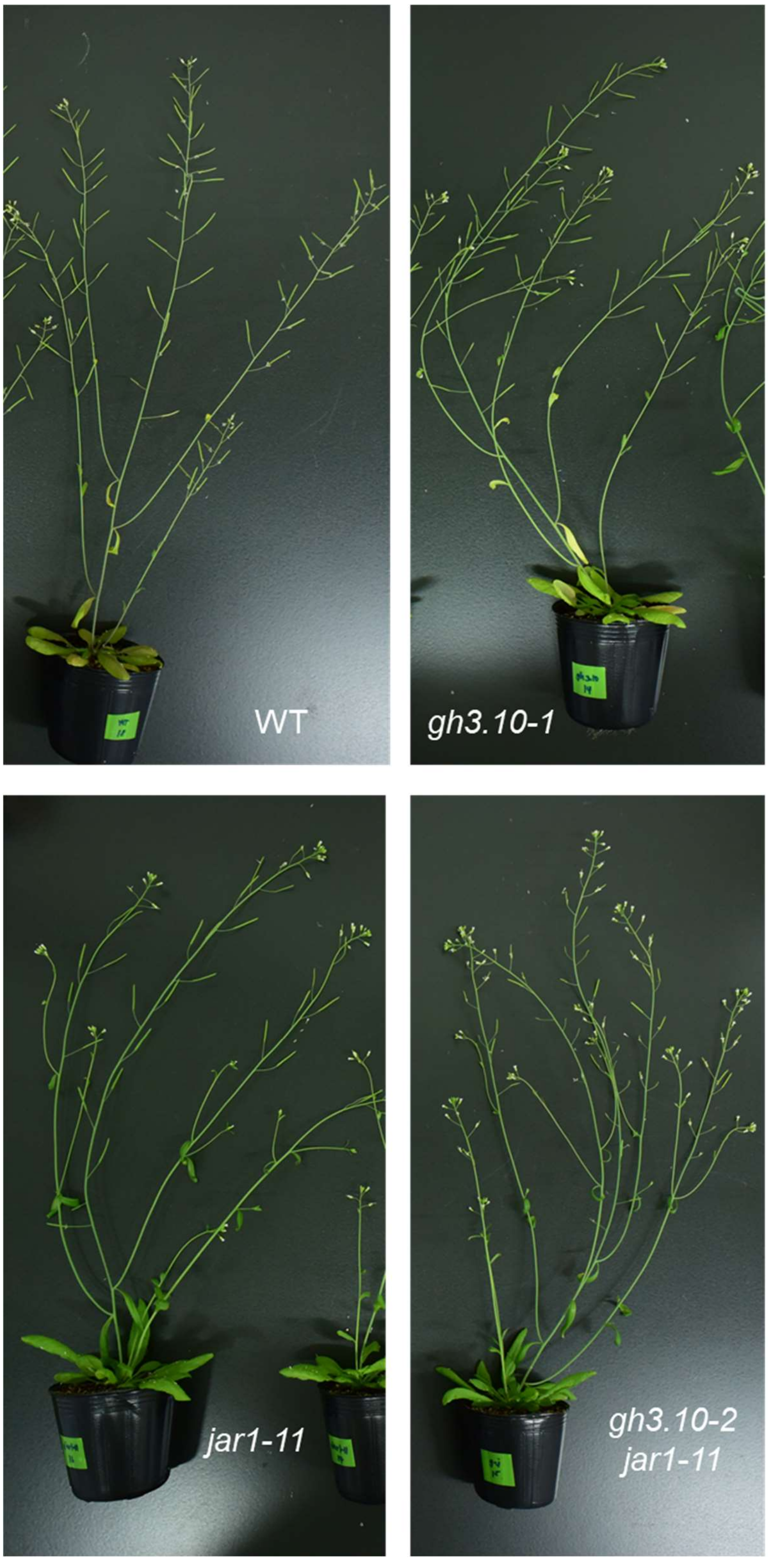

Figure 15. *GH3.10* and *JAR1* Arabidopsis mutants 42 days after germination

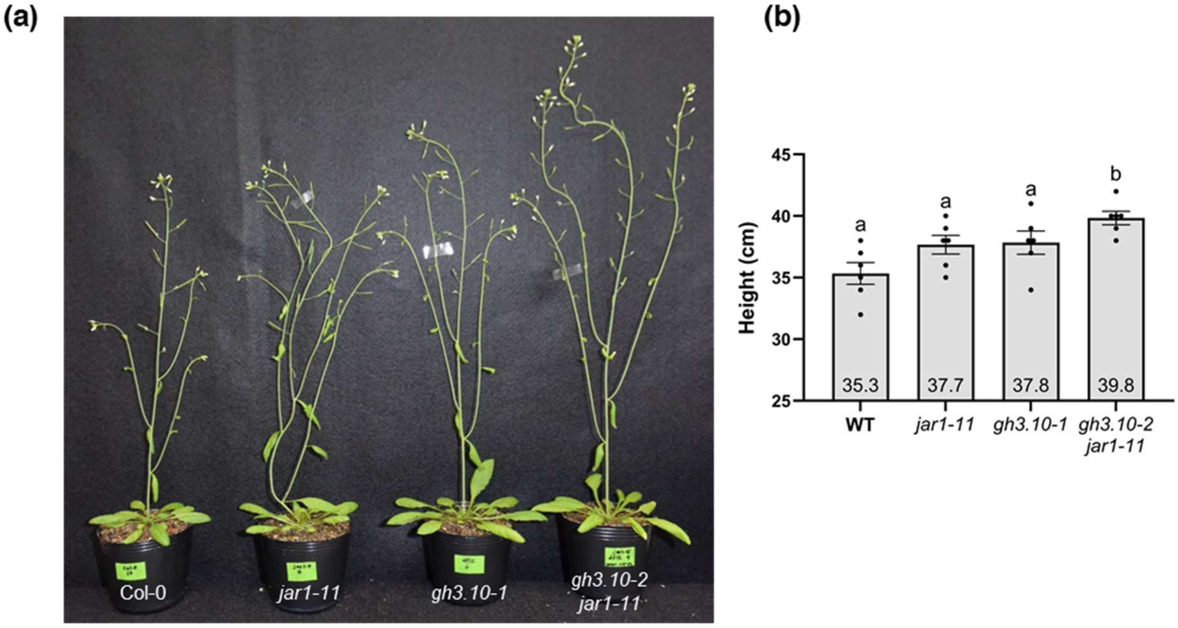

Figure 16. Growth of *GH3.10* and *JAR1* mutants

(a) Representative WT, *jar1-11*, *gh3.10-1*, and *gh3.10-2 jar1-11* Arabidopsis plants 45 days after germination. **(b)** Lengths of 42-day-old plants, measured from the root-stem junction to the tip of the main inflorescence (n = 6). Different letters indicate statistical difference by one-way ANOVA with Tukey HSD (p<0.05).

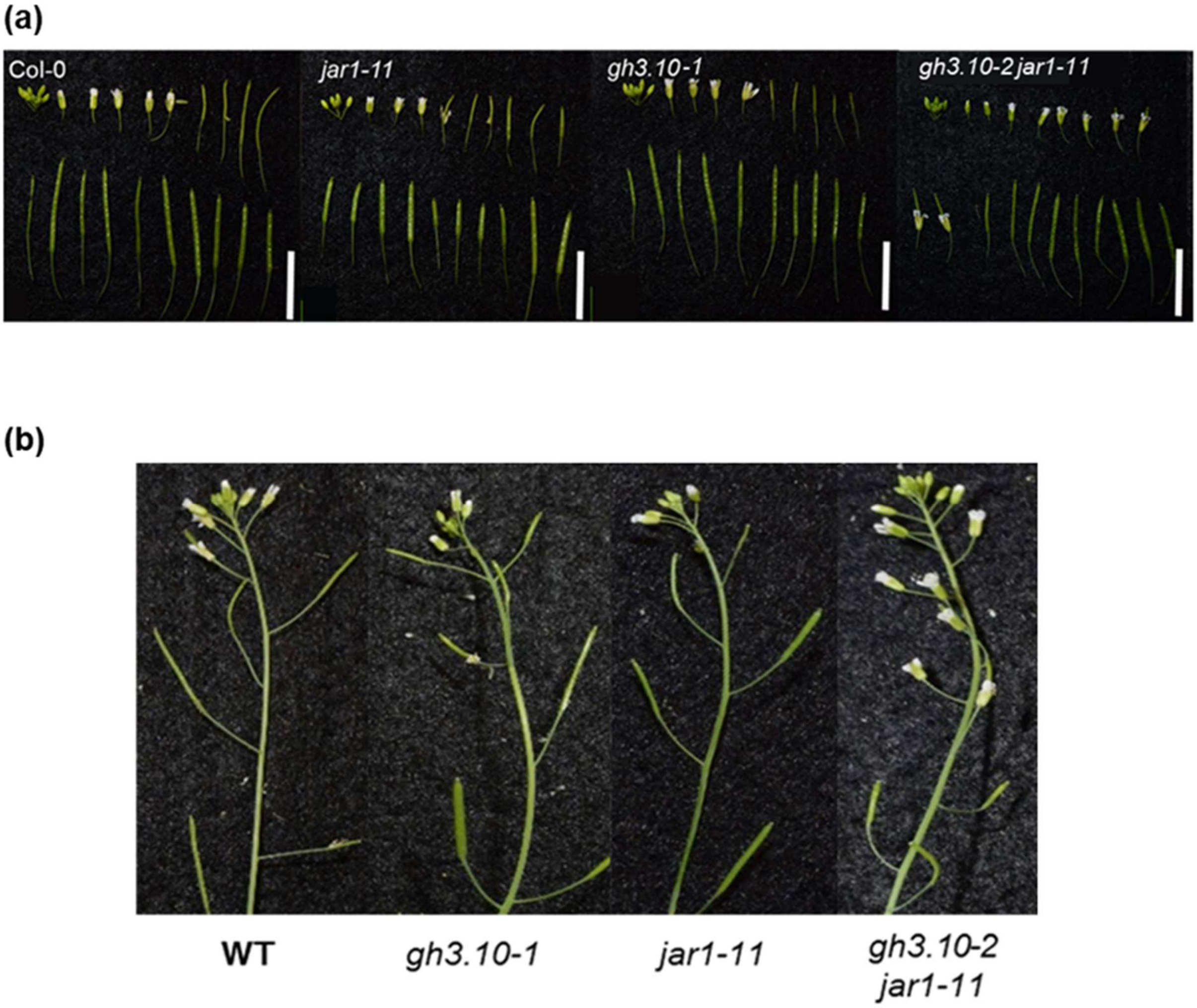

Figure 17. Flower-to-silique transition in *GH3.10* and *JAR1* mutants

(a) Flower buds, flowers, and siliques from the main inflorescence of representative plants of each genotype (bar = 1 cm). **(b)** Representative flower inflorescences of WT and mutant plants 75 days after germination.

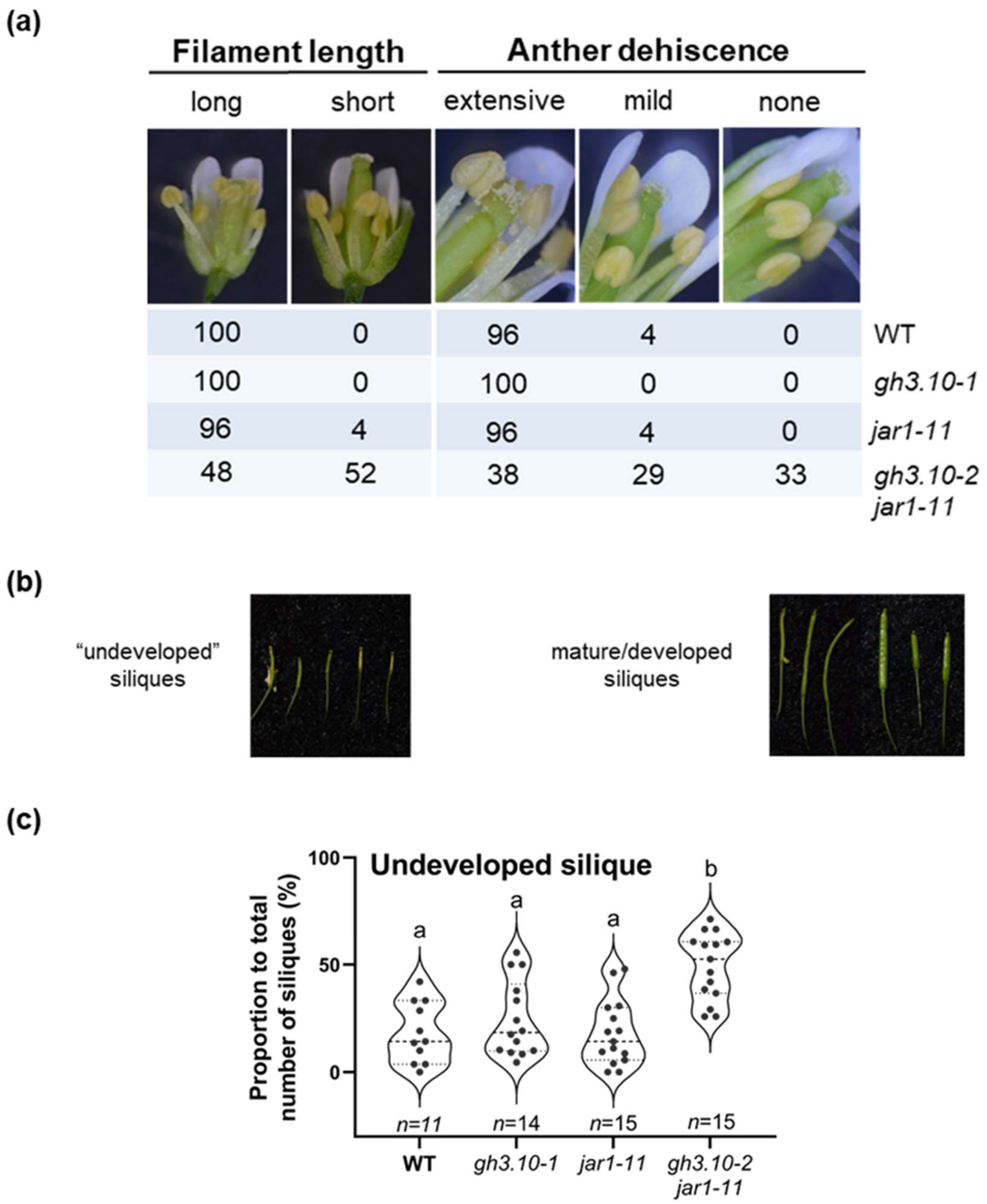

	long	short	extensive	mild	none
WT	100	0	96	4	0
gh3.10-1	100	0	100	0	0
jar1-11	96	4	96	4	0
gh3.10-2 jar1-11	48	52	38	29	33

Figure 18. Stamen and silique development in *JAR1-GH3.10* mutants

(a) Prevalence (in percentage) of the stamen filament lengths and degrees of anther dehiscence in stage 14 flowers. Fewer than three dehisced anthers in a flower was characterized here as mild. For each genotype, 21-24 flowers from different inflorescences were examined. (b) Representative siliques that were considered as undeveloped or mature/developed. "Undeveloped" siliques include those that failed to develop seeds and the immature ones that might or might not eventually bear seeds (bar = 1 cm). (c) Proportion (in percentage) of undeveloped siliques observed in the main inflorescences. Different lowercase letters indicate significant difference based on ANOVA with Tukey HSD (p<0.05).

(a)

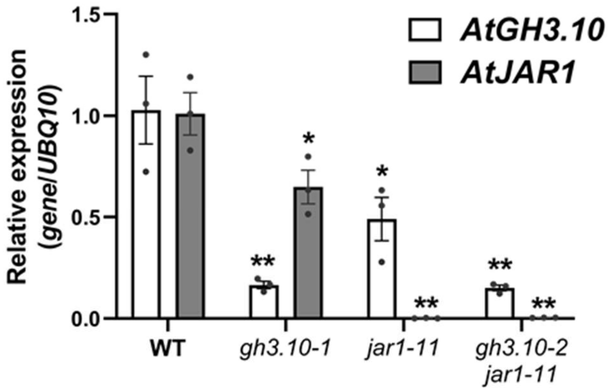

(b)

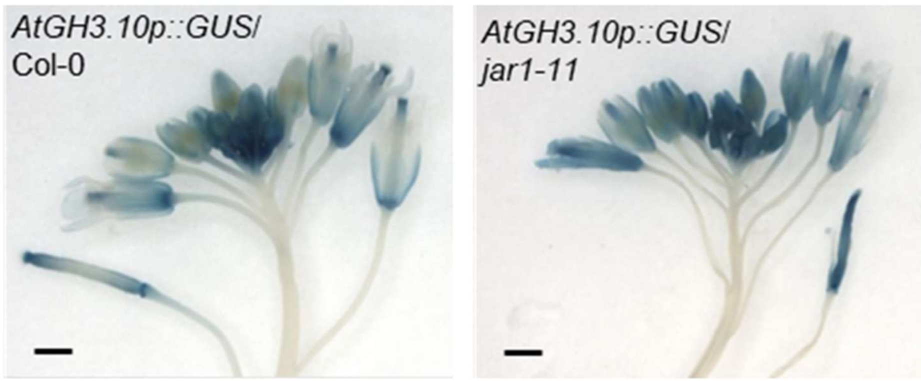

Figure 19. Expression of *AtH3.10* and *AtJAR1* in the flowers

(a) Relative expression of *AtGH3.10* and *AtJAR1* in the flower buds of mutant plants relative to WT. Values were standardized to *UBQ10* and expressed as fold difference relative to WT. Each bar represents the mean of three biological replicates. Asterisks indicate significant difference with the respective WT by Dunnett's *t*-test (**p*<0.05, ***p*<0.01). (b) Localization of *AtGH3.10* promoter:GUS activity in the flower buds and siliques of WT and *jar1-11* plants (bar = 1 mm).

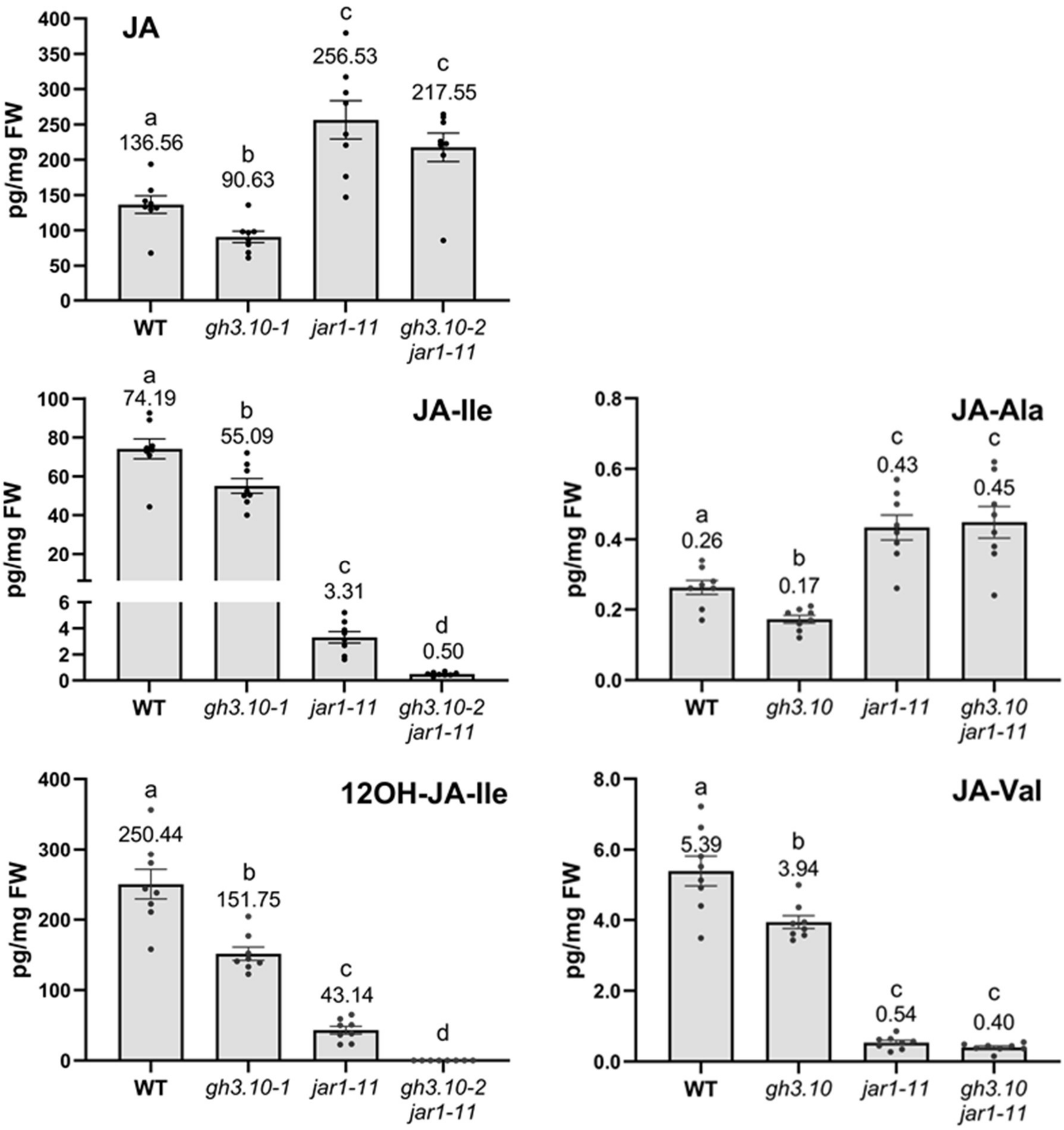

Figure 20. JA and JA-amino acid conjugates in the flower buds

Levels of JA and JA-amido conjugates in the flower bud clusters of 40-day-old Arabidopsis plants. Different lowercase letters indicate statistical difference by one-way ANOVA with Games-Howell test (p<0.05). Values are mean of eight biological replicates ± SEM. Limit of quantitation (LOQ) (in pg/mg FW, based on minimum plant weight used): 0.12 (JA), 0.04 (JA-Ile), 0.81 (12OH-JA-Ile), 0.06 (JA-Ala and JA-Val).

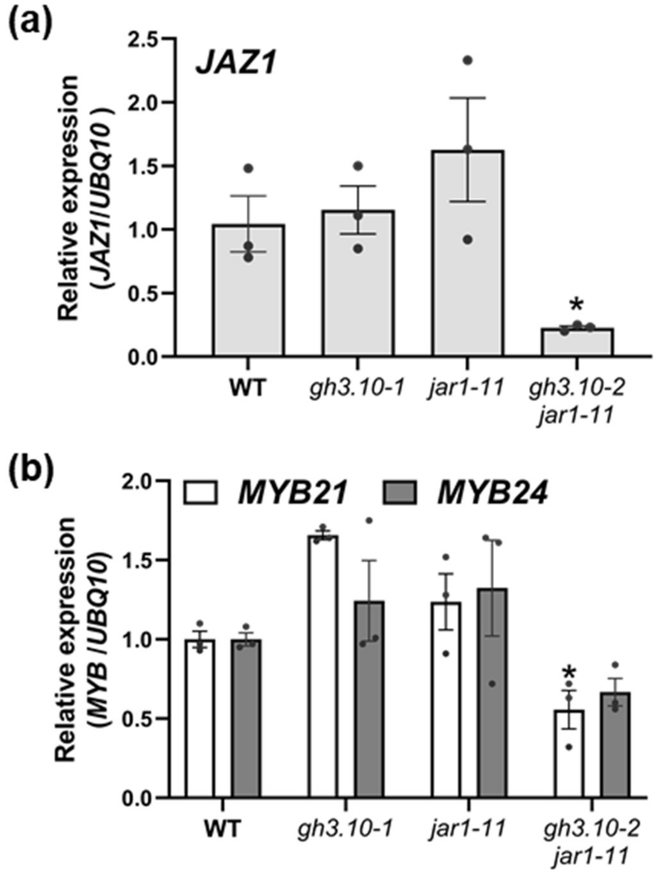

Figure 21. Expression of JA- and floral development-related genes

(a) Relative expression of *JAZ1*, a transcriptional repressor of JA-response genes, in the flower buds of mutants compared to WT. (b) Gene expression levels of *MYB21* and *MYB24* in the flower buds. Values in B and C are the means of three replicates, each comprised of pooled samples from at least three independent plants with error bars indicating the SEM. Asterisks indicate significant differences compared to WT by ANOVA with Dunnett's *t*-test (p<0.05).

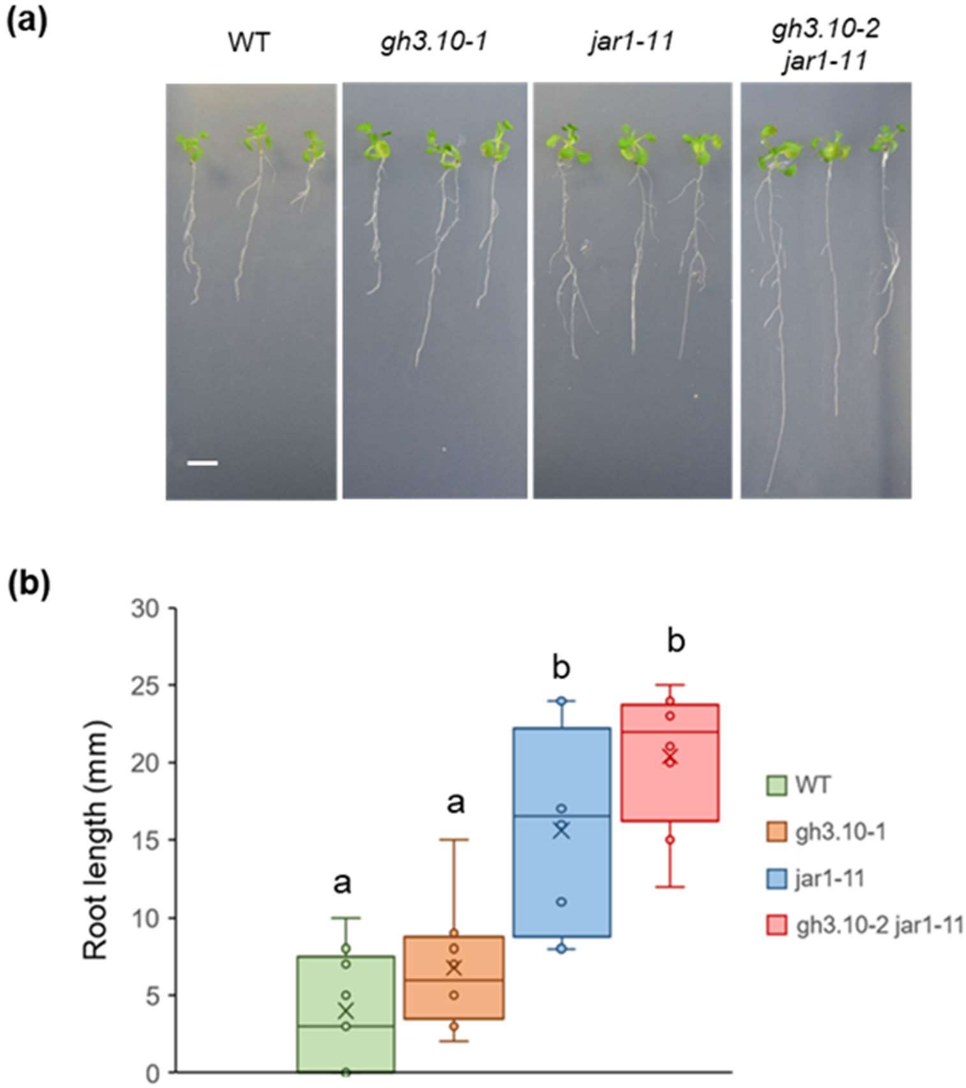

Figure 22. Effect of exogenous JA treatment in root growth of *AtGH3.10* and *AtJAR1* mutants

(a) Root growth of *AtJAR1* and *AtGH3.10* Arabidopsis mutants on ½ MS medium supplemented with 5 μM JA. Scale bar = 5 mm. (b) Root lengths of the sampled plants including those in (a). Horizontal line within a box indicates the median while X marks the mean of *n*=8-9 measurements. Top and bottom error bars indicate the maximum and minimum values, respectively.

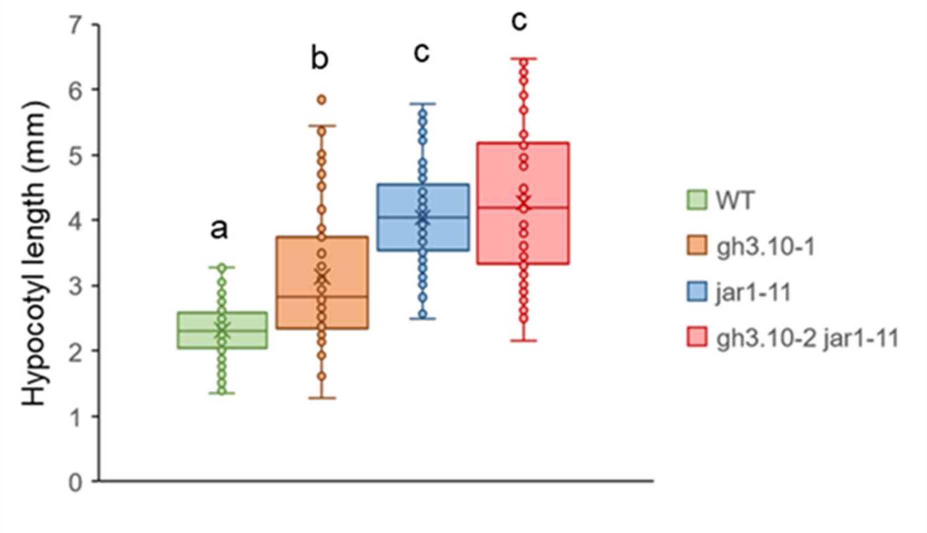

Figure 23. Effect of red-light treatment in hypocotyl growth of *AtGH3.10* and *AtJAR1* mutants

Hypocotyl elongation under continuous red light. Different lowercase letters above the error bars in (b) and (c) indicate significant difference at $p<0.05$ by ANOVA with Tukey HSD and at p<0.000 by Kruskal Wallis Test adjusted by Bonferroni correction, respectively.

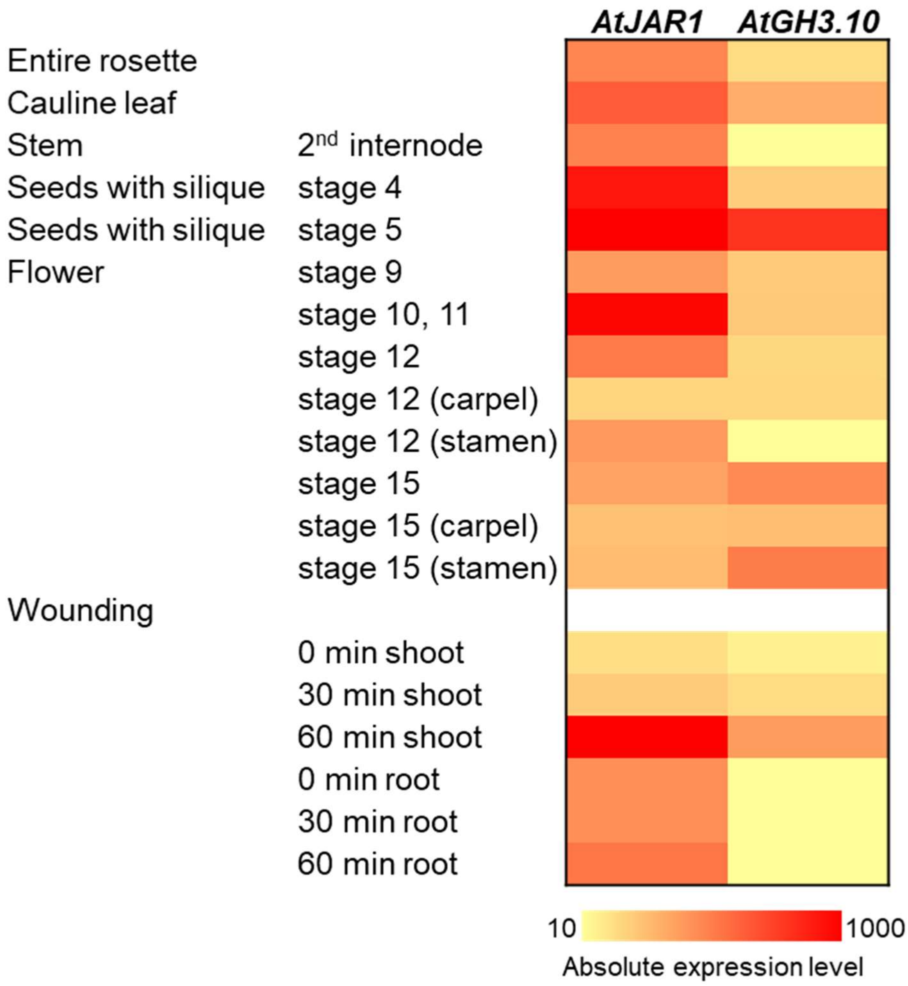

Figure 24. Expression of *AtJAR1* and *AtGH3.10* in Arabidopsis

Colors indicate the absolute gene expression values in Col-0 Arabidopsis plant. Data was obtained from Arabidopsis eFP Browser. (http://bar.utoronto.ca/efp/cgi-bin/efpWeb.cgi).

DISCUSSION

1.0 Phylogenetic origin of *AtGH3.10*

For the past two decades, the existence of an Arabidopsis enzyme capable of conjugating JA and amino acids aside from JAR1 has been suspected since the *jar1* mutants have moderate phenotypes. The other enzyme that biosynthesizes JA-Ile had remained elusive since the biochemical activity of AtGH3.10, the closest enzyme candidate, had not been determined (Staswick *et al.*, 2002; Staswick and Tiryaki, 2004; Chiu *et al.*, 2018). To this end, this study has functionally characterized AtGH3.10 as another JA-amido synthetase in *A. thaliana*.

The long evolutionary origin of *AtGH3.10*-like sequences inferred from the phylogeny shown in Fig. 5 suggests divergence from *AtJAR1*-like sequences when flowering plants emerged from an ancestral vascular plant, thereby creating two previously reported subgroups (Okrent and Wildermuth, 2011). The *AtGH3.10*-like sequences eventually dispersed across the angiosperm lineage but diversified only among eudicots, while the gene remained fundamentally conserved in the monocot lineage until the emergence of grasses (Poaceae family). This apparent loss of *AtGH3.10*-like sequences in the Poaceae coincided with the whole genome duplication event that occurred in the taxon (Freeling, 2009).

2.0 Enzymatic activity of AtGH3.10

For the first time since the functional characterization of AtJAR1 two decades ago, the enzymatic activity of AtGH3.10 has finally been shown in this study after previous attempts were unsuccessful in demonstrating the enzyme's *in vitro* activity. The elusiveness of AtGH3.10's activity in enzyme assays might be due to the enzyme's susceptibility to degradation as some researchers believed (Bottcher *et al.*, 2015). The ability of recombinant AtGH3.10 to synthesize the bioactive form of JA-Ile conclusively demonstrated that the enzyme is a JA-Ile synthetase that is similar to AtJAR1. As shown by LC-MS/MS analysis, the main reaction product of AtGH3.10 and AtJAR1 was a mixture of (+)-*cis*-JA-Ile and (–)-*trans*-JA-Ile (Fig. 6b,c). In terms of substrate affinity, the relatively lower K_m value of AtJAR1 to JA compared to AtGH3.10 (Table 1) is indicative of AtJAR1's preference for JA as its primary substrate. In contrast, the lower JA-binding capacity of AtGH3.10 might be a reflection of the structural difference in its acyl binding site with that of AtJAR1 (Westfall *et al.*, 2012) as a probable consequence of their long history of divergence (Fig. 5). While the recombinant AtGH3.10 exhibited comparable degrees of specific activities for both JA and Ile substrates, the recombinant AtJAR1 showed a lower specific activity in Ile-limited condition than in JA-limited condition (Table 1). In connection with this, differences in JA-amino acid synthetic activities were observed between the recombinant AtGH3.10 and AtJAR1, such that AtGH3.10 was more receptive to other amino acids than AtJAR1 at least *in vitro* (Fig. 7c). JA-Ala, JA-Leu, JA-Met, and JA-Val can also promote COI1-JAZ interaction to varying degrees *in vitro* (Thines *et al.*, 2007; Katsir *et al.*, 2008). Although those JA-amino acid conjugates can promote the binding of COI1 and JAZ proteins isolated from Arabidopsis and tomato, their interaction with two rice COI1s (OsCOI1a and OsCOI1b) was lost or was appreciably weaker compared to OsCOI2, a functional homolog of COI1 (Thines *et al.*, 2007; Katsir *et al.*, 2008; Yan *et al.*, 2016). Although further investigation is needed to understand COI-dependent jasmonate signaling in rice, it is intriguing that the absence of *AtGH3.10*-like sequences in grasses is coincidental with the differential affinity of OsCOIs for JA-amino acids, considering that the preference of AtGH3.10 for the four amino acids was suggested by our study.

3.0 AtGH3.10 and the plant wound response

JA-Ile is usually maintained at low levels unless inductive factors such as abiotic and biotic stresses are present (Suza and Staswick, 2008). The expression of *AtGH3.10* was induced by wounding like *AtJAR1* but it differed notably in that the former was induced later than 30 minutes (Fig. 9a). The contribution of *AtGH3.10* in JA-Ile biosynthesis upon wounding was hardly revealed by the instantaneous levels of JA-Ile at 30- and 120-minute time points but it was reflected in the levels of 12OH-JA-Ile. Though the highest amount of JA-Ile observed in *jar1-11* was only about 4 pg/mg FW, there were about 100 and 1,800 pg/mg FW of the 12OH-JA-Ile that accumulated in *jar1-11* by 30 and 120 minutes after wounding (Fig. 11). Since 12OH-JA-Ile can only be derived from JA-Ile based on our current understanding of JAs metabolism (Wasternack and Feussner, 2018; Fig. 1), the substantial amount of 12OH-JA-Ile observed in *jar1-11* was likely in the form of JA-Ile sometime before 120 minutes following wounding, which could thereby represent the least amount of bioactive JA that AtGH3.10 was producing. Nevertheless, it has been shown that 12OH-JA-Ile itself is slightly bioactive (Jimenez-Aleman *et al.*, 2019; Poudel *et al.*, 2019). It is also important to emphasize that both JA-Ile and 12OH-JA-Ile could be catabolized into yet other forms of JAs (Wasternack and Feussner, 2018) and thus the biosynthetic contribution of *AtGH3.10* described in this study is only partial. Taking this into account, the function of *AtGH3.10* in *jar1-11* seemed sufficient to elicit the expression of *OPR3* and *JAZ1* to the same extent as that of *AtJAR1* in *gh3.10-1* (Fig. 9b). On the other hand, since *jar1* implies that only a relatively lower levels of bioactive JAs were needed to elicit a wound response (Fig. 9 and 11), it appears that Arabidopsis tends to biosynthesize JA-Ile profusely upon stress exposure. The excess production of bioactive JAs during wound stress might be necessary for the plant's immunity to subsequent stress. In fact, derivatives of JA-Ile accumulate within the leaf midveins following wound stress that might be needed for the distal transport of signals and consequent induction of a systemic response (Glauser *et al.*, 2008). Consistent to this, the eventual decline of JA-Ile levels in the leaves by 120 minutes post wounding was concurrent with the abrupt accumulation of 12OH-JA-Ile (Fig. 11). Furthermore, the observed systemic induction of *AtGH3.10* expression and consequent accumulation of bioactive JAs proved this point (Fig. 13, Fig. 14).

4.0 AtGH3.10 and flower development

JA-Ile appeared to accumulate more in the flower buds of mature plants than in the leaves under normal conditions (Fig. 11, Fig. 20). In both plant organs, the amount of JA-Ile was far less in *jar1-11* than in *gh3.10-1*. Additionally, the *AtJAR1* is expressed higher in rosette leaves, flower tissues younger than stage 12, and wounded leaves than *AtGH3.10* (Fig. 24). These observations suggest that AtJAR1 is the primary producer of JA-Ile and that AtGH3.10 contributes comparatively less (at least in the aforementioned plant parts), although the recombinant AtGH3.10 outperformed AtJAR1 in *in vitro* reactions (Fig. 7c, Table 1). On the other hand, *AtGH3.10* and *AtJAR1* had differential effects on JA levels in the flower buds of single mutants (Fig. 20). As further studies focusing on overall signaling and metabolism of JA in different tissues are needed, the differential effect on JA level might be due to the functional difference between *AtGH3.10* and *AtJAR1* in influencing the signaling process to induce JA biosynthesis and catabolism, or to a possible metabolic pathway preferentially mediated by *AtGH3.10*. Meanwhile, rendering the two JA-amido synthetases non-functional in *gh3.10-2 jar1-11* did not eliminate the hormone, and residual amounts of JA-Ile, JA-Ala, and JA-Val were still produced in the flower buds and wounded leaves. This finding suggests that the conjugation of JA to amino acids could be catalyzed by yet other enzymes that might be promiscuous members of the GH3 protein family. Indeed, some of the members of group II GH3 enzymes (Fig. 2) that have known activities on auxin could also conjugate amino acids to JA (Gutierrez *et al.*, 2012). These multiple sources of bioactive JAs in Arabidopsis add to the inherent redundancy in jasmonate signaling processes, *e.g.*, there are 13 *JAZ* genes in Arabidopsis that have varying and overlapping interaction specificities to different transcription factors and have differential spatiotemporal expression patterns (Chini *et al.*, 2016; Guo *et al.*, 2018).

The amounts of JA-Ile in *jar1-11* and *gh3.10-2 jar1-11* were significantly low compared to that in WT. Even though the difference in JA-Ile level between *jar1-11* and *gh3.10-2 jar1-11* was relatively small (Fig. 20), the *jar1-11* still displayed normal flower phenotype while the *gh3.10-2 jar1-11* showed significant number of non-fertile flowers (Fig. 17a,b; Fig. 18a). This observation can be explained by the considerable amount of 12OH-JA-Ile that was detected in the flower buds of *jar1-11* but not in *gh3.10-2 jar1-11* (Fig. 20), which might mean that a substantial amount of JA-Ile was initially present in *jar1-11* that had activated JA signaling before being catabolized into its hydroxylated form. Although the hydroxylation of JA-Ile is implicated in the inactivation of the hormone (Koo *et al.*, 2011; Heitz *et al.*, 2012), the 12OH-JA-Ile could still promote COI1 and JAZ interaction *in vitro* and is still bioactive to some extent (Jimenez-Aleman *et al.*, 2019; Poudel *et al.*, 2019). On the other hand, the *gh3.10-2 jar1-11* still showed partial flower fertility that might be attributed to the presence of low levels of JA-Ile, JA-Ala, and JA-Val that could altogether activate COI1-mediated signaling for reproductive development, thereby allowing some flowers to develop successfully into siliques with viable seeds (Fig. 17, Fig. 18). This is in contrast to the full flower sterile phenotype of *opr2-1 opr3-3* mutant that is devoid of JA-Ile due to its inability to produce JA (Chini *et al.*, 2018). Additionally, it is possible that the hormone production (like the low amounts of JAs in *gh3.10-2 jar1-11*), is localized to specific floral tissues that might be critical in maintaining the flower fertility; this could be elucidated by the application of highly sensitive hormone quantitation methods such as single-cell mass spectrometry (Shimizu *et al.*, 2015).

Another aspect that underlies the partial fertility of *gh3.10-2 jar1-11* is the transcriptional regulation related to flower development. Stunted stamen filaments were present in about 50 percent of *gh3.10-2 jar1-11* flowers and about 60 percent of the flowers had anthers that dehisced mildly or not at all (Fig. 18a). These phenotypes are similar to the hallmarks of the *myb21 myb24* double knockout, which also includes reduced male fertility (Mandaokar *et al.*, 2006). Both MYB21 and MYB24 are required for normal stamen development and are JA-responsive since they are subject to JAZ repression via direct interactions (Song *et al.*, 2011). The decrease in *MYB21* expression in *gh3.10-2 jar1-11* (Fig. 21b) exemplifies the JA-mediated regulation of flower development. Additionally, despite the attenuated *JAZ1* expression in *gh3.10-2 jar1-11* (Fig. 21a), other JAZ proteins such as JAZ8, JAZ10, and JAZ11 could still repress MYB21/24 (Song *et al.*, 2011), not to mention that the regulation of JAZ8 is COI1-independent (Shyu *et al.*, 2012). The compromised MYB21 level, compounded by possible repression by other JAZ proteins, partly explain the reduced fertility in *gh3.10-2 jar1-11*.

5.0 AtGH3.10 and plant growth

One important aspect of *AtGH3.10* functions is its inhibitory effect on the elongation of hypocotyl under red light (Takase *et al.*, 2003). This light-dependent response is shared by *AtJAR1* as similar phenotype could be observed in *jar1* grown in far-red and low fluence red light (Chen *et al.*, 2007; Wang *et al.*, 2011).

The observed retardation of hypocotyl elongation in *gh3.10-1*, *jar1-11*, and *gh3.10-2 jar1-11* under continuous red light (Fig. 23) further proves the shared physiological function of the two enzymes. The mechanism how JAs might be involved in photomorphogenesis and the crosstalk of JA and light signaling pathways are subjects of many ongoing research efforts.

CONCLUSIONS AND RECOMMENDATIONS

The central role of JA-Ile in JA-mediated processes makes the study of its biosynthesis and metabolic fate extremely important for understanding how jasmonates mediate some aspects of plant development and stress responses. Additionally, identifying the molecular players that are redundantly involved in some branches of the JA-signaling pathways (*e.g.*, the contributing sources of bioactive JAs) could be instrumental for elucidating the roles of other diverse jasmonate derivatives.

To this end, this study has demonstrated that AtGH3.10 is another JA-amido synthetase, in addition to AtJAR1, that had long been speculated to biosynthesize JA-Ile and other JA-amino acid conjugates in Arabidopsis. The study further showed that the relatively small amount of endogenous JA-amido conjugates that AtGH3.10 could produce was sufficient to sustain normal flower development to considerable extent and to elicit the JA-associated responses to wound stress even in the absence of AtJAR1. Additionally, insights into the evolutionary history and distribution of *AtGH3.10* orthologs across plant taxa were provided which might hold clues of the possible sub-functionalization of the gene. Further investigations aimed at other probable acyl acid substrates, tissue-level expressions under various stress conditions, and temporal metabolism of JAs at a global scale may reveal a distinct role for *AtGH3.10* in plants.

ACKNOWLEDGMENTS

This research was done with the contributions of Yuri Kanno and Mitsunori Seo at RIKEN Center for Sustainable Resource Science (Kanagawa, Japan) who performed the quantitation of hormones, Naoki Kitaoka and Hideyuki Matsuura at Hokkaido University (Division of Fundamental AgriScience Research, Research Faculty of Agriculture, Sapporo, Japan) who provided valuable advice and the hormone standards, and Takayuki Tohge and Takafumi Shimizu at NAIST who served as the advisers. Funding was supported by NAIST, JSPS KAKENHI Grant-in-Aid for Young Scientists (18K14398), and Scientific Research B (19H03249) and C (19K06723). Special thanks are also extended to Mutsumi Watanabe (NAIST) for advice and to the Japanese Government (MEXT) for scholarship.

REFERENCES

Bottcher, C., Burbidge, C.A., di Rienzo, V., Boss, P.K. & Davies, C. (2015) Jasmonic acid-isoleucine formation in grapevine (*Vitis vinifera* L.) by two enzymes with distinct transcription profiles. *Journal of Integrative Plant Biology*, 57(7), 618-627.

Chen, H.J., Fu, T.Y., Yang, S.L. & Hsieh, H.L. (2018) FIN219/JAR1 and cryptochrome1 antagonize each other to modulate photomorphogenesis under blue light in Arabidopsis. *PLoS Genet*, 14, e1007248.

Chen, I.C., Huang, I.C., Liu, M.J., Wang, Z.G., Chung, S.S. & Hsieh, H.L. (2007) Glutathione S-transferase interacting with far-red insensitive 219 is involved in phytochrome A-mediated signaling in Arabidopsis. *Plant Physiology*, 143, 1189-1202.

Chini, A., Fonseca, S., Fernández, G., Adie, B., Chico, J.M., Lorenzo, O. *et al.* (2007) The JAZ family of repressors is the missing link in jasmonate signalling. *Nature*, 448, 666-671.

Chini, A., Gimenez-Ibanez, S., Goossens, A. & Solano, R. (2016) Redundancy and specificity in jasmonate signalling. *Current Opinion in Plant Biology*, 33, 147-156.

Chini, A., Monte, I., Zamarreño, A.M., Hamberg, M., Lassueur, S., Reymond, P. *et al.* (2018) An OPR3-independent pathway uses 4,5-didehydrojasmonate for jasmonate synthesis. *Nature Chemical Biology*, 14, 171-178.

Chiu, L.W., Heckert, M.J., You, Y., Albanese, N., Fenwick, T., Siehl, D.L. *et al.* (2018) Members of the GH3 family of proteins conjugate 2,4-D and dicamba with aspartate and glutamate. *Plant and Cell Physiology*, 59, 2366-2380.

Chung, H.S., Koo, A.J., Gao, X., Jayanty, S., Thines, B., Jones, A.D. *et al.* (2008) Regulation and function of Arabidopsis JASMONATE ZIM-domain genes in response to wounding and herbivory. *Plant Physiology*, 146, 952-964.

Creelman, R.A. & Mullet, J.E. (1997) Biosynthesis and action of jasmonates in plants. *Annual Review of Plant Physiology Plant Molecular Biology*, 48, 355-381.

Ferrari, S., Plotnikova, J.M., De Lorenzo, G. & Ausubel, F.M. (2003) Arabidopsis local resistance to *Botrytis cinerea* involves salicylic acid and camalexin and requires EDS4 and PAD2, but not SID2, EDS5 or PAD4. *The Plant Journal*, 35, 193-205.

Fonseca, S., Chini, A., Hamberg, M., Adie, B., Porzel, A., Kramell, R. *et al.* (2009) (+)-7-iso-Jasmonoyl-L-isoleucine is the endogenous bioactive jasmonate. *Nature Chemical Biology*, 5, 344-350.

Freeling, M. (2009) Bias in plant gene content following different sorts of duplication: tandem, whole-genome, segmental, or by transposition. *Annual Review of Plant Biology*, 60, 433-453.

Glauser, G., Grata, E., Dubugnon, L., Rudaz, S., Farmer, E.E. & Wolfender, J.L. (2008) Spatial and temporal dynamics of jasmonate synthesis and accumulation in Arabidopsis in response to wounding. *Journal of Biological Chemistry*, 283, 16400-16407.

Guo, Q., Yoshida, Y., Major, I.T., Wang, K., Sugimoto, K., Kapali, G. *et al.* (2018) JAZ repressors of metabolic defense promote growth and reproductive fitness in. *Proceedings of the National Academy of Sciences of the United States of America*, 115, E10768-E10777.

Gutierrez, L., Mongelard, G., Flokova, K., Pacurar, D., Novak, O., Staswick, P. *et al.* (2012) Auxin controls Arabidopsis adventitious root initiation by regulating jasmonic acid homeostasis. *The Plant Cell,* 24(6), 2515-2527.

Heitz, T., Widemann, E., Lugan, R., Miesch, L., Ullmann, P., Desaubry, L. *et al.* (2012) Cytochrome P450 CYP94C1 and CYP94B3 catalyze two successive oxidation steps of plant hormone jasmonoyl-isoleucine for catabolic turnover. *Journal of Biological Chemistry*, 287(9), 6296-6306.

Howe, G.A., Major, I.T. & Koo, A.J. (2018) Modularity in Jasmonate Signaling for Multistress Resilience. *Annual Review of Plant Biology*, 69, 387-415.

Jimenez-Aleman, G.H., Almeida-Trapp, M., Fernandez-Barbero, G., Gimenez-Ibanez, S., Reichelt, M., Vadassery, J. *et al.* (2019) Omega hydroxylated JA-Ile is an endogenous bioactive jasmonate that signals through the canonical signaling pathway. *Biochimica et Biophysica Acta - Molecular and Cell Biology of Lipids*, 1864(158520).

Kanno, Y., Oikawa, T., Chiba, Y., Ishimaru, Y., Shimizu, T., Sano, N. *et al.* (2016) AtSWEET13 and AtSWEET14 regulate gibberellin-mediated physiological processes. *Nature Communications*, 7, 13245.

Katsir, L., Schilmiller, A.L., Staswick, P.E., He, S.Y. & Howe, G.A. (2008) COI1 is a critical component of a receptor for jasmonate and the bacterial virulence factor coronatine. *Proceedings of the National Academy Sciences of the United States of America*, 105, 7100-7105.

Koo, A.J., Cooke, T.F. & Howe, G.A. (2011) Cytochrome P450 CYP94B3 mediates catabolism and inactivation of the plant hormone jasmonoyl-L-isoleucine. *Proceedings of the National Academy of Sciences of the United States of America*, 108, 9298-9303.

Koo, A.J., Gao, X., Daniel, J.A., & Howe, G.A. (2009) A rapid wound signal activates the systemic synthesis of bioactive jasmonates in Arabidopsis. *The Plant Journal* 59: 974-986.

Koo, A.J. & Howe, G.A. (2009) The wound hormone jasmonate. *Phytochemistry*, 70, 1571-1580.

Koo, A.J., Thireault, C., Zemelis, S., Poudel, A.N., Zhang, T., Kitaoka, N. *et al.* (2014) Endoplasmic reticulum-associated inactivation of the hormone jasmonoyl-L-isoleucine by multiple members of the cytochrome P450 94 family in Arabidopsis. *Journal of Biological Chemistry*, 289(43), 29728-29738.

Mandaokar, A., Thines, B., Shin, B., Lange, B.M., Choi, G., Koo, Y.J. *et al.* (2006) Transcriptional regulators of stamen development in Arabidopsis identified by transcriptional profiling. *The Plant Journal*, 46, 984-1008.

Meesters, C., Mönig, T., Oeljeklaus, J., Krahn, D., Westfall, C.S., Hause, B. *et al.* (2014) A chemical inhibitor of jasmonate signaling targets JAR1 in Arabidopsis thaliana. *Nature Chemical Biology*, 10, 830-836.

Miersch, O., Neumerkel, J., Dippe, M., Stenzel, I. & Wasternack, C. (2008) Hydroxylated jasmonates are commonly occurring metabolites of jasmonic acid and contribute to a partial switch-off in jasmonate signaling. *New Phytologist*, 177, 114-127.

Motohashi, K. (2015) A simple and efficient seamless DNA cloning method using SLiCE from *Escherichia coli* laboratory strains and its application to SLiP site-directed mutagenesis. *BMC Biotechnology*, 15, 47.

Okrent, R.A., Brooks, M.D. & Wildermuth, M.C. (2009) Arabidopsis GH3.12 (PBS3) conjugates amino acids to 4-substituted benzoates and is inhibited by salicylate. *Journal of Biological Chemistry*, 284, 9742-9754.

Okrent, R.A. & Wildermuth, M.C. (2011) Evolutionary history of the GH3 family of acyl adenylases in rosids. *Plant Molecular Biology*, 76, 489-505.

Park, J.H., Halitschke, R., Kim, H.B., Baldwin, I.T., Feldmann, K.A. & Feyereisen, R. (2002) A knock-out mutation in allene oxide synthase results in male sterility and defective wound signal transduction in Arabidopsis due to a block in jasmonic acid biosynthesis. *The Plant Journal*, 31, 1-12.

Pratiwi, P., Tanaka, G., Takahashi, T., Xie, X., Yoneyama, K., Matsuura, H. *et al.* (2017) Identification of jasmonic acid and jasmonoyl-isoleucine, and characterization of AOS, AOC, OPR and AtJAR1 in the model lycophyte *Selaginella moellendorffii*. *Plant and Cell Physiology,* 58, 789-801.

Poudel, A.N., Holtsclaw, R.E., Kimberlin, A., Sen, S., Zeng, S., Joshi, T. *et al.* (2019) 12-Hydroxy-jasmonoyl-L-isoleucine is an active jasmonate that signals through CORONATINE INSENSITIVE1 and contributes to the wound response in Arabidopsis. *Plan and Cell Physiology*, 60(10), 2152-2166.

Riemann, M., Riemann, M., & Takano, M. (2008) Rice JASMONATE RESISTANT1 is involved in phytochrome and jasmonate signalling. *Plant Cell and Environment*, 31(6), 783-792.

Sheard, L.B., Tan, X., Mao, H., Withers, J., Ben-Nissan, G., Hinds, T.R. *et al.* (2010) Jasmonate perception by inositol-phosphate-potentiated COI1-JAZ co-receptor. *Nature*, 468, 400-405.

Shimizu, T., Miyakawa, S., Esaki, T., Mizuno, H., Masujima, T., Koshiba, T. *et al.* (2015) Live single-cell plant hormone analysis by video-mass spectrometry. *Plant and Cell Physiology*, 56, 1287-1296.

Shimizu, T., Miyamoto, K., Minami, E., Nishizawa, Y., Iino, M., Nojiri, H. *et al.* (2013) OsJAR1 contributes mainly to biosynthesis of the stress-induced jasmonoyl-isoleucine involved in defense responses in rice. *Bioscience Biotechnology and Biochemistry*, 77, 1556-1564.

Shyu, C., Figueroa, P., Depew, C.L., Cooke, T.F., Sheard, L.B., Moreno, J.E. *et al.* (2012) JAZ8 lacks a canonical degron and has an EAR motif that mediates transcriptional repression of jasmonate responses in Arabidopsis. *The Plant Cell*, 24, 536-550.

Smyth, D.R., Bowman, J.L. & Meyerowitz, E.M. (1990) Early flower development in Arabidopsis. *The Plant Cell*, 2, 755-767.

Song, S., Qi, T., Huang, H., Ren, Q., Wu, D., Chang, C. *et al.* (2011) The Jasmonate-ZIM domain proteins interact with the R2R3-MYB transcription factors MYB21 and MYB24 to affect Jasmonate-regulated stamen development in Arabidopsis. *The Plant Cell*, 23, 1000-1013.

Staswick, P.E., Serban, B., Rowe, M., Tiryaki, I., Maldonado, M.T., Maldonado, M.C. *et al.* (2005) Characterization of an Arabidopsis enzyme family that conjugates amino acids to indole-3-acetic acid. *The Plant Cell*, 17, 616-627.

Staswick, P.E., Su, W. & Howell, S.H. (1992) Methyl jasmonate inhibition of root growth and induction of a leaf protein are decreased in an Arabidopsis thaliana mutant. *Proceedings of the National Academy of Sciences of the United States of America*, 89, 6837-6840.

Staswick, P.E. & Tiryaki, I. (2004) The oxylipin signal jasmonic acid is activated by an enzyme that conjugates it to isoleucine in Arabidopsis. *The Plant Cell*, 16, 2117-2127.

Staswick, P.E., Tiryaki, I. & Rowe, M.L. (2002) Jasmonate response locus JAR1 and several related Arabidopsis genes encode enzymes of the firefly luciferase superfamily that show activity on jasmonic, salicylic, and indole-3-acetic acids in an assay for adenylation. *The Plant Cell*, 14, 1405-1415.

Suza, W.P. & Staswick, P.E. (2008) The role of JAR1 in Jasmonoyl-L: -isoleucine production during Arabidopsis wound response. *Planta*, 227, 1221-1232.

Suza WP, Rowe ML, Hamberg M & Staswick PE. (2010) A tomato enzyme synthesizes (+)-7-iso-jasmonoyl-L-isoleucine in wounded leaves. *Planta,* 231, 717-728.

Takase, T., Nakazawa, M., Ishikawa, A., Manabe, K. & Matsui, M. (2003) DFL2, a new member of the Arabidopsis GH3 gene family, is involved in red light-specific hypocotyl elongation. *Plant and Cell Physiology*, 44, 1071-1080.

Thines, B., Katsir, L., Melotto, M., Niu, Y., Mandaokar, A., Liu, G. *et al.* (2007) JAZ repressor proteins are targets of the SCF(COI1) complex during jasmonate signalling. *Nature*, 448, 661-665.

Tsutsui, H. & Higashiyama, T. (2017) pKAMA-ITACHI vectors for highly efficient CRISPR/Cas9-mediated gene knockout in Arabidopsis thaliana. *Plant and Cell Physiology*, 58, 46-56.

Wakuta, S., Suzuki, E., Saburi, W., Matsuura, H., Nabeta, K., Imai, R. *et al.* (2011) OsJAR1 and OsJAR2 are jasmonoyl-L-isoleucine synthases involved in wound- and pathogen-induced jasmonic acid signalling. *Biochemical and Biophysical Research Communications,* 409(4), 634-639.

Wang, J.G., Chen, C.H., Chien, C.T. & Hsieh, H.L. (2011) FAR-RED INSENSITIVE219 modulates CONSTITUTIVE PHOTOMORPHOGENIC1 activity via physical interaction to regulate hypocotyl elongation in Arabidopsis. *Plant Physiology*, 156, 631-646.

Wasternack C, & Feussner I. (2018) The oxylipin pathways: Biochemistry and function. *Annual Review of Plant Biology,* 69, 363-386.

Wasternack, C. & Hause, B. (2013) Jasmonates: biosynthesis, perception, signal transduction and action in plant stress response, growth and development. An update to the 2007 review in Annals of Botany. *Annals of Botany*, 111, 1021-1058.

Westfall, C.S., Zubieta, C., Herrmann, J., Kapp, U., Nanao, M.H. & Jez, J.M. (2012) Structural basis for prereceptor modulation of plant hormones by GH3 proteins. *Science*, 336, 1708-1711.

Widemann, E., Miesch, L., Lugan, R., Holder, E., Heinrich, C., Aubert, Y. *et al.* (2013) The amidohydrolases IAR3 and ILL6 contribute to jasmonoyl-isoleucine hormone turnover and generate 12-hydroxyjasmonic acid upon wounding in Arabidopsis leaves. *Journal of Biological Chemistry*, 288(44), 31701-31714.

Wojtaczka, P., Ciarkowska, A., Starzynska, E., & Ostrowski, M. (2022) The GH3 amidosynthetases family and their role in metabolic crosstalk modulation of plant signaling compounds. *Phytochemistry*, 194, 113039.

Xie, D.X., Feys, B.F., James, S., Nieto-Rostro, M. & Turner, J.G. (1998) COI1: an Arabidopsis gene required for jasmonate-regulated defense and fertility. *Science*, 280, 1091-1094.

Yan, J., Li, S., Gu, M., Yao, R., Li, Y., Chen, J. *et al.* (2016) Endogenous bioactive jasmonate is composed of a set of (+)-7-*iso*-JA-amino acid conjugates. *Plant Physiology*, 172, 2154-2164.

Yan, Y., Stolz, S., Chetelat, A., Reymond, P., Pagni, M., Dubugnon, L. *et al.* (2007) A downstream mediator in the growth repression limb of the jasmonate pathway. *The Plant Cell*, 19(8), 2470-2483.

Yoshihara, T., Omer, E., Koshino, H., Sakamura, S., Kikuta, Y. & Koda, Y. (1989) Structure of a tuber-Inducing stimulus from potato leaves (*Solanum tuberosum* L.). *Agricultural and Biological Chemistry*, 53, 2835-2837.